Combining squark production and decay at NLO QCD

in collaboration with Wolfgang Hollik and Davide Pagani
based on
arXiv:1207.1071 & arXiv:1303.0186

University of Zurich[UZH]

LHCphenOnet

Jonas M. Lindert
University of Zurich

LHCPhenoNet annual meeting
CERN, 5th December 2013

The MSSM

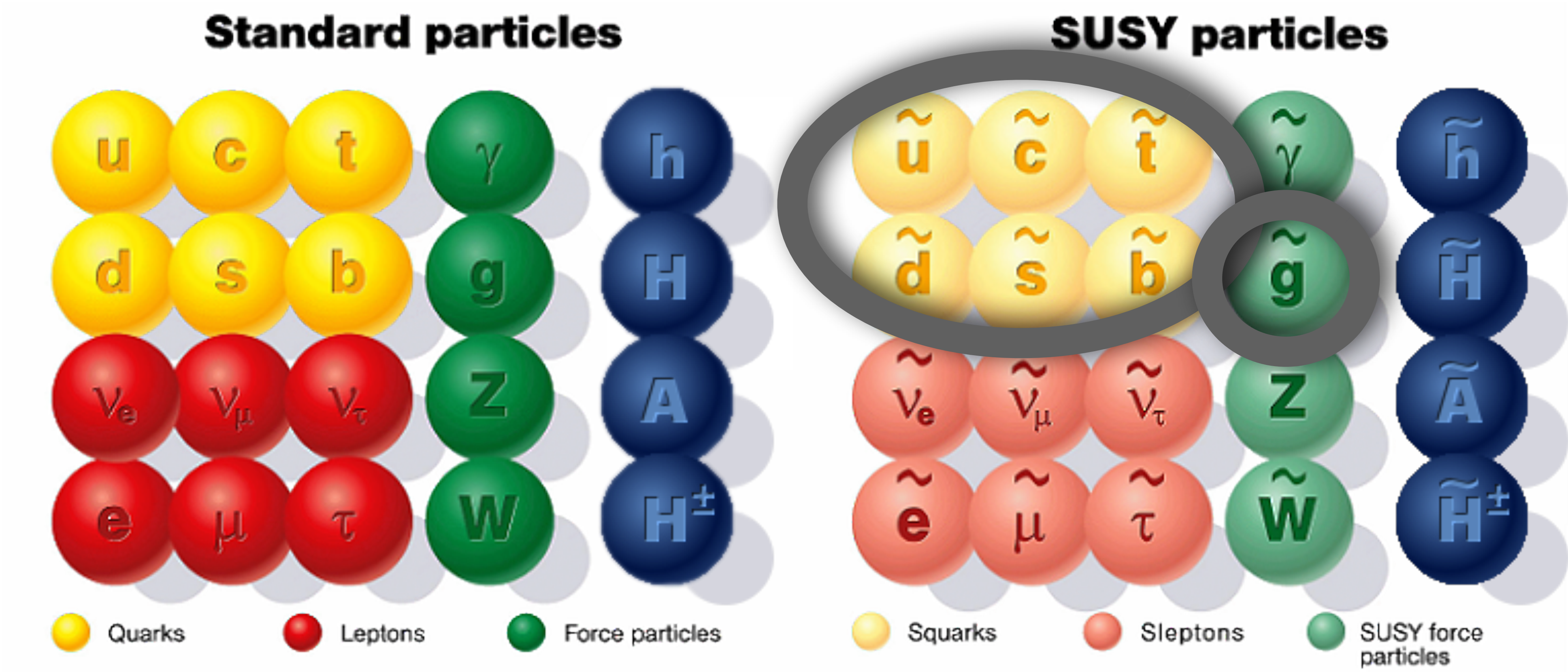

Often the lightest neutralino assumed to be the (stable) LSP ➜ missing Energy + DM

e.g.

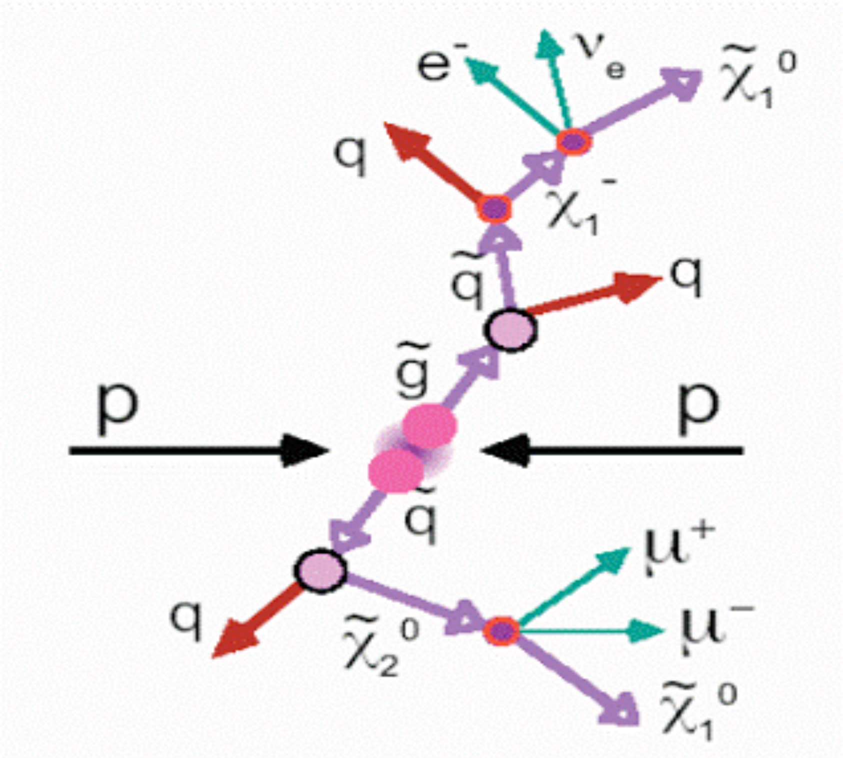

but also:

- more or less jets
- more or less leptons
- b-tagged jets

in general

- many particles in the final state

Squarks and gluinos at the LHC

EXCLUSION LIMITS

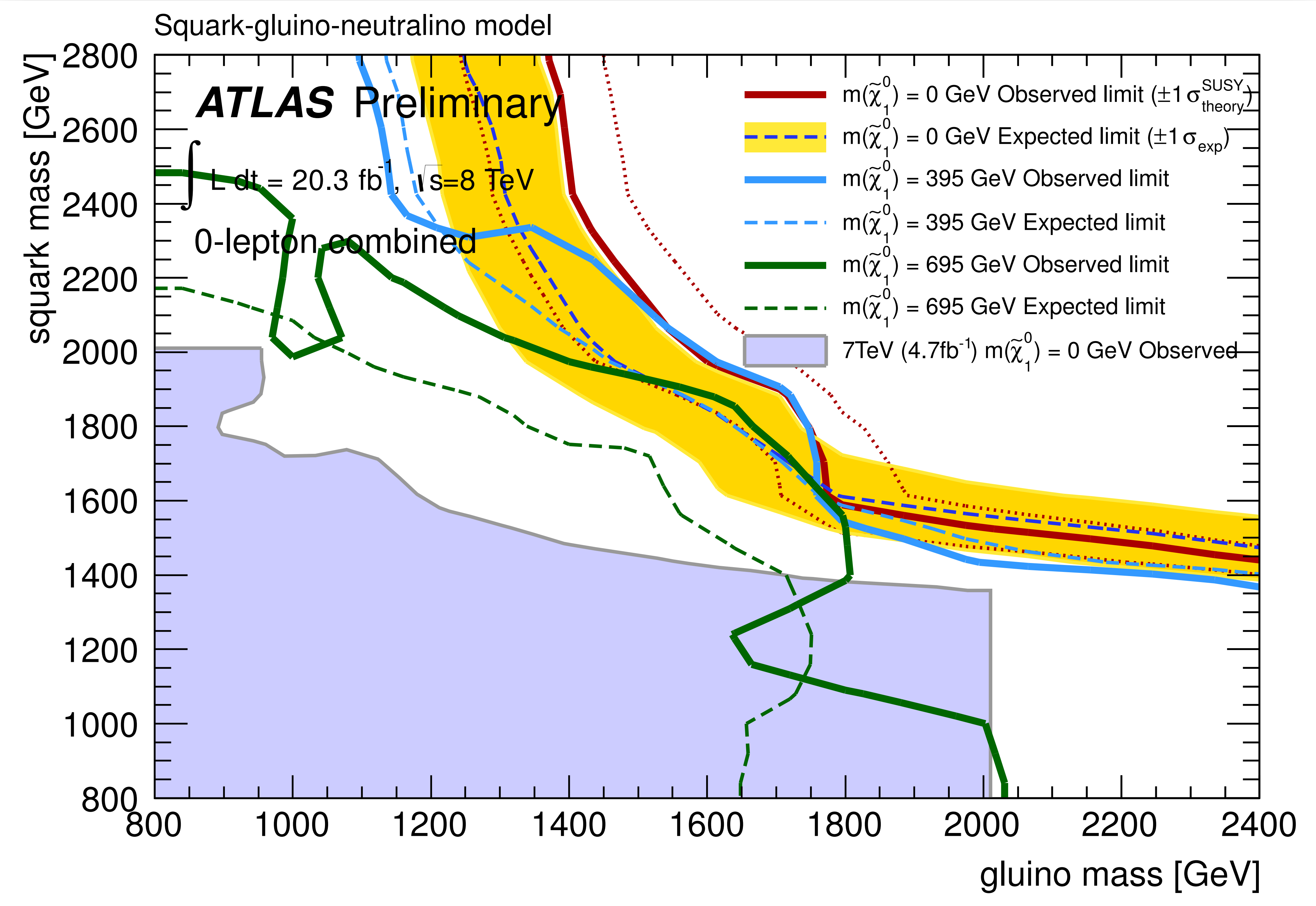

Squarks and gluinos at the LHC

EXCLUSION LIMITS

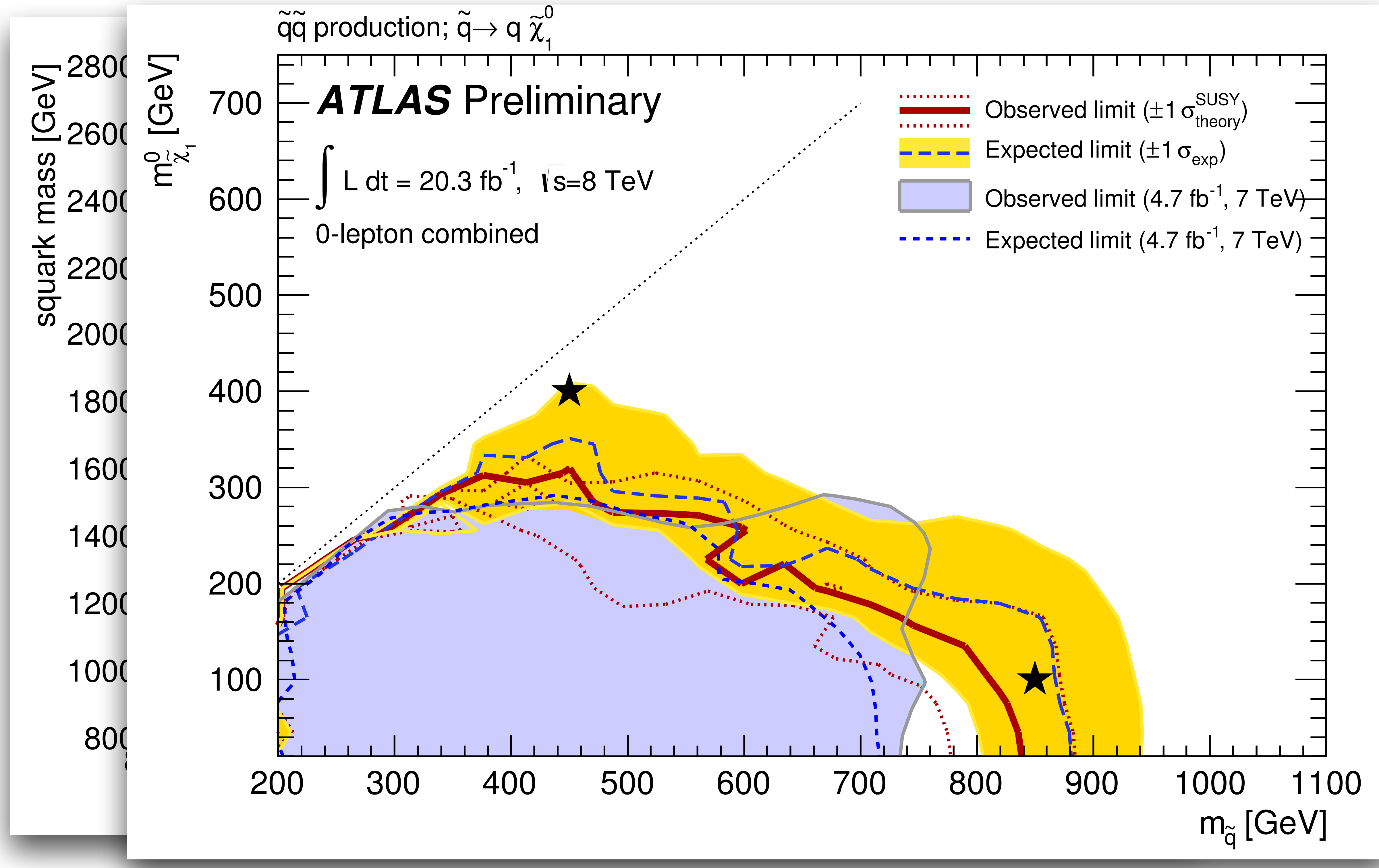

Why higher orders?

Corrections can be large!

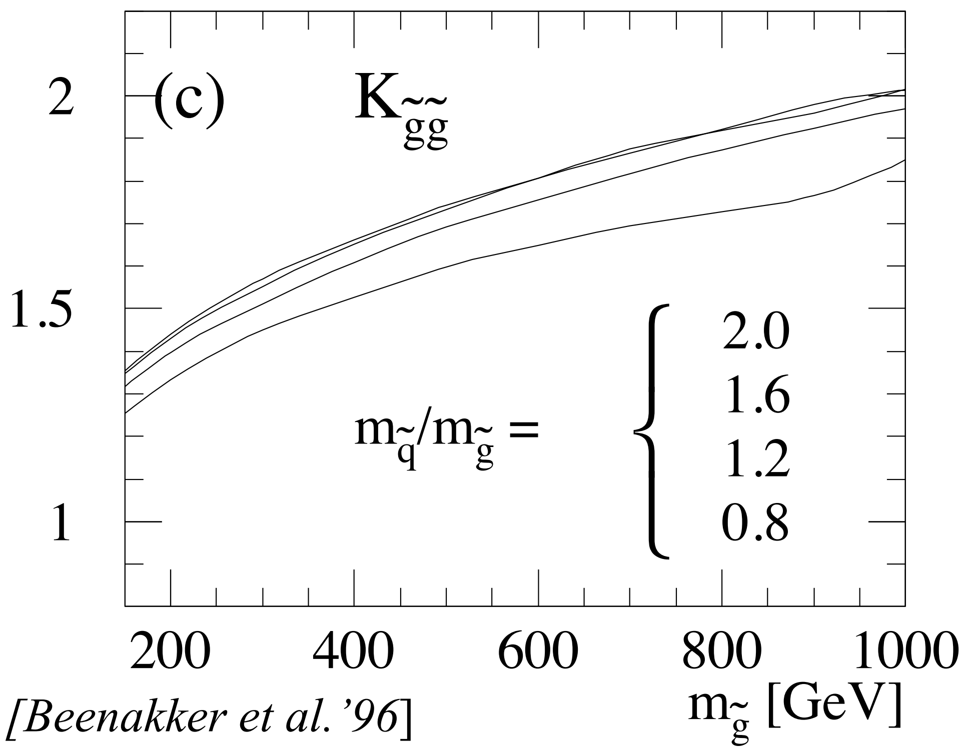

[Beenakker et al.'96]

Accurate exclusion limits.

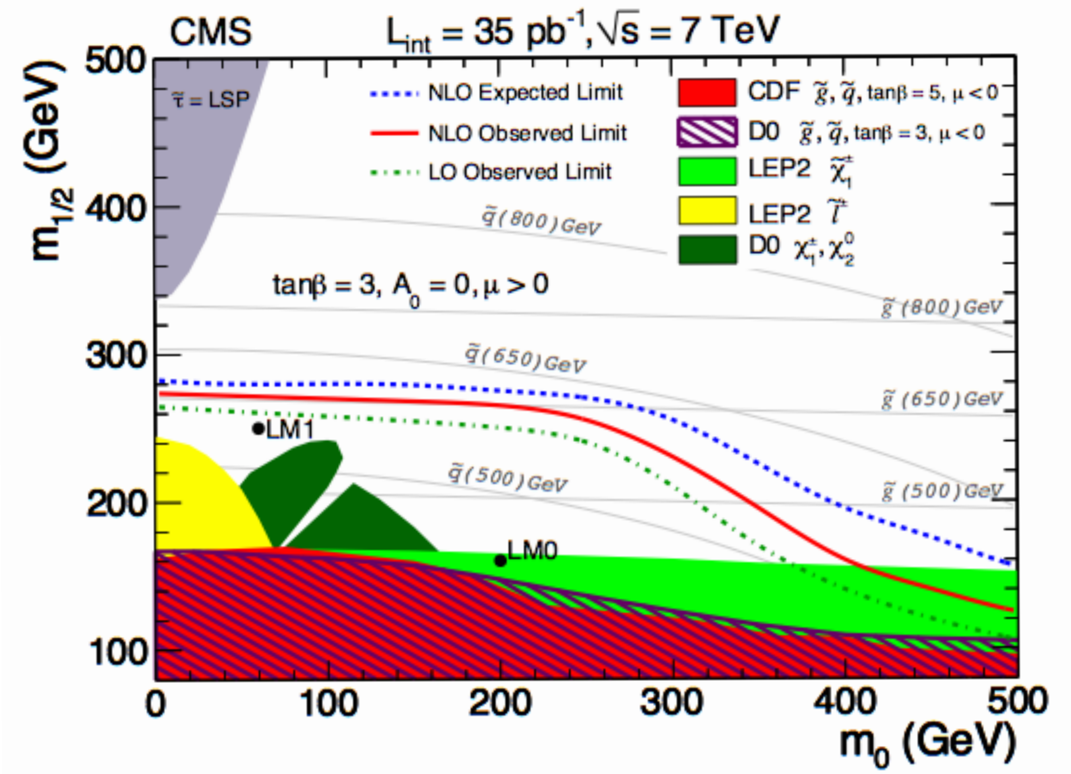

Study & reduce theoretical uncertainties.

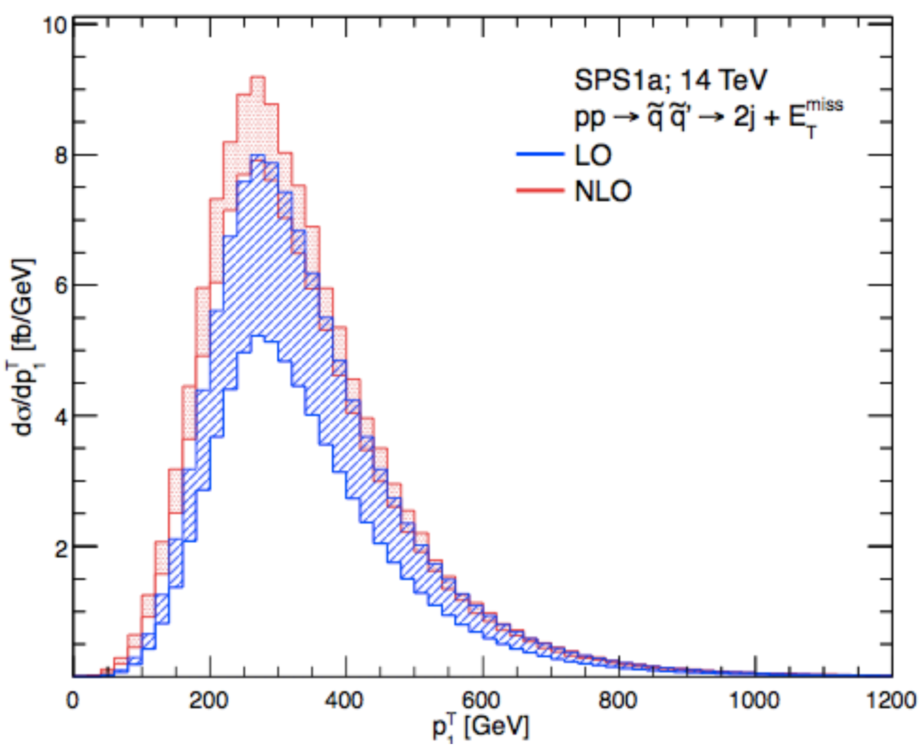

Necessary for parameter determination.

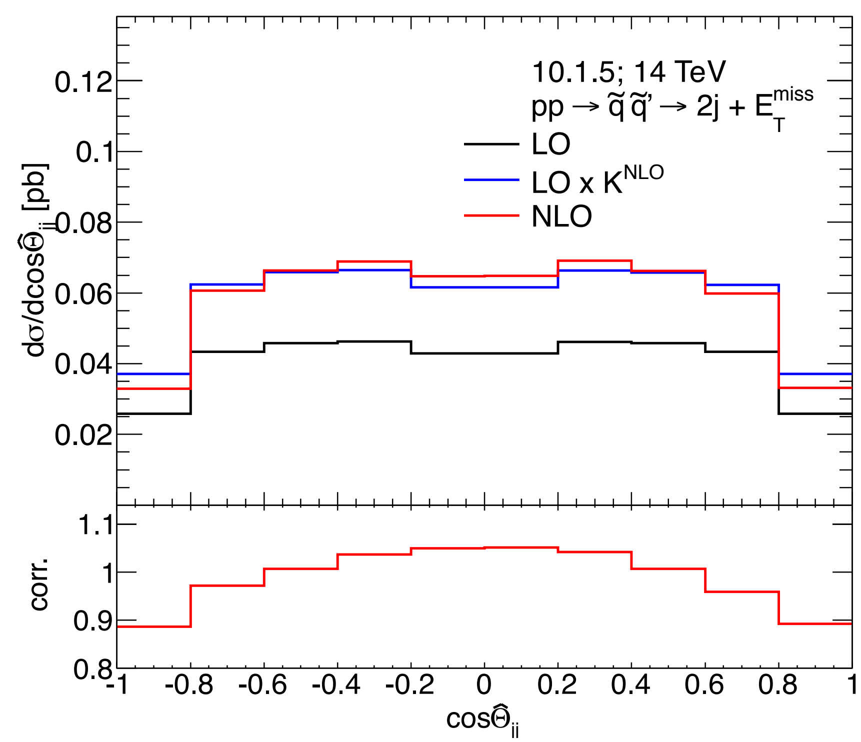

Squarks at the LHC

Production

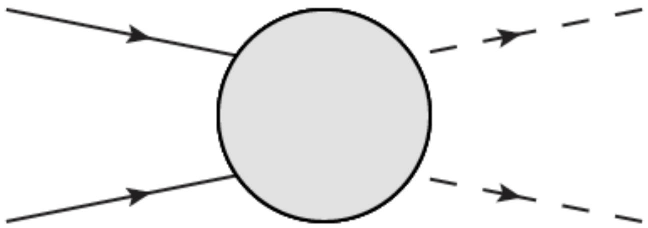

Squark-Squark production:
LO QCD: *Baer, Tata '85*
NLO QCD: *Beenakker, Höpker, Spira, Zerwas '96*
Tool: PROSPINO2 (inclusive), *Plehn et. al.*
Automatization: *Goncalves-Netto et al. '12*
LO EW: *Bornhauser, Drees, Dreiner, Kim* '07
NLO EW: *Germer, Hollik, Mirabella, Trenkel '10*
Beyond NLO (resummed):
Beenakker et al. '09 & '11 (soft)
Falgari, Schwinn, Wever '12 + '13 (soft+coulomb)
POWHEG-BOX: *Gavin et. al. '13*

Decay

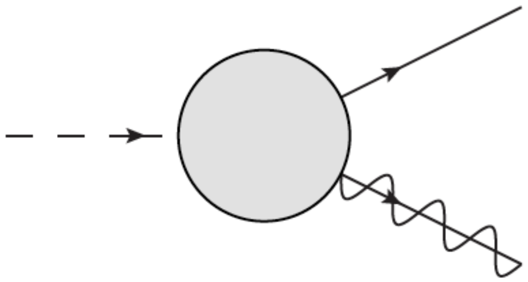

Squark decay:
NLO QCD: *Djouadi, Hollik, Jünger '96*
Tool: SDECAY (integrated widths),
Mühlleitner, Djouadi, Mambrini
NLO EW: *Guasch, Hollik, Sola '02*

NLO QCD to EW decay chain:
Horsky, *Krämer, Mück, Zerwas '08*

Higher-order corrections are generally large for inclusive cross sections.

Differential distributions at NLO in terms of experimental signatures have not been studied.

For a systematic treatment at NLO production and decays have to be combined.

Combining production and direct decay at NLO

We study the experimental signature $2j + \not{E}_T(+X)$

via squark-squark production and direct decay into the lightest neutralino. $pp \to \tilde{q}\tilde{q}' \to qq'\tilde{\chi}_1^0\tilde{\chi}_1^0(+X)$

Full LO process

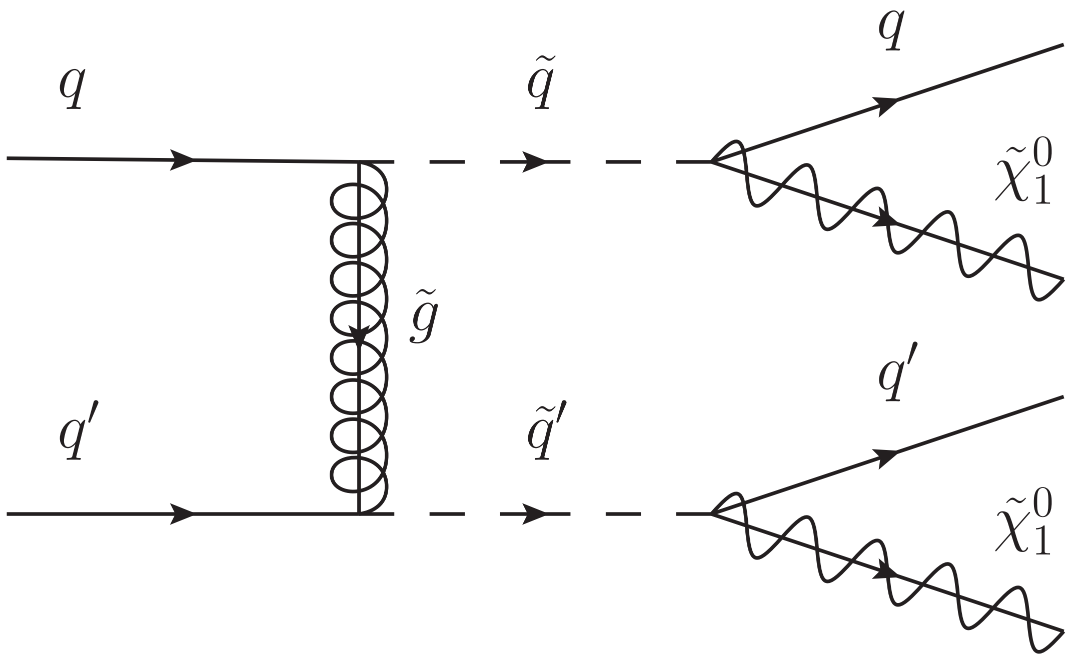

Why squark-squark channel?

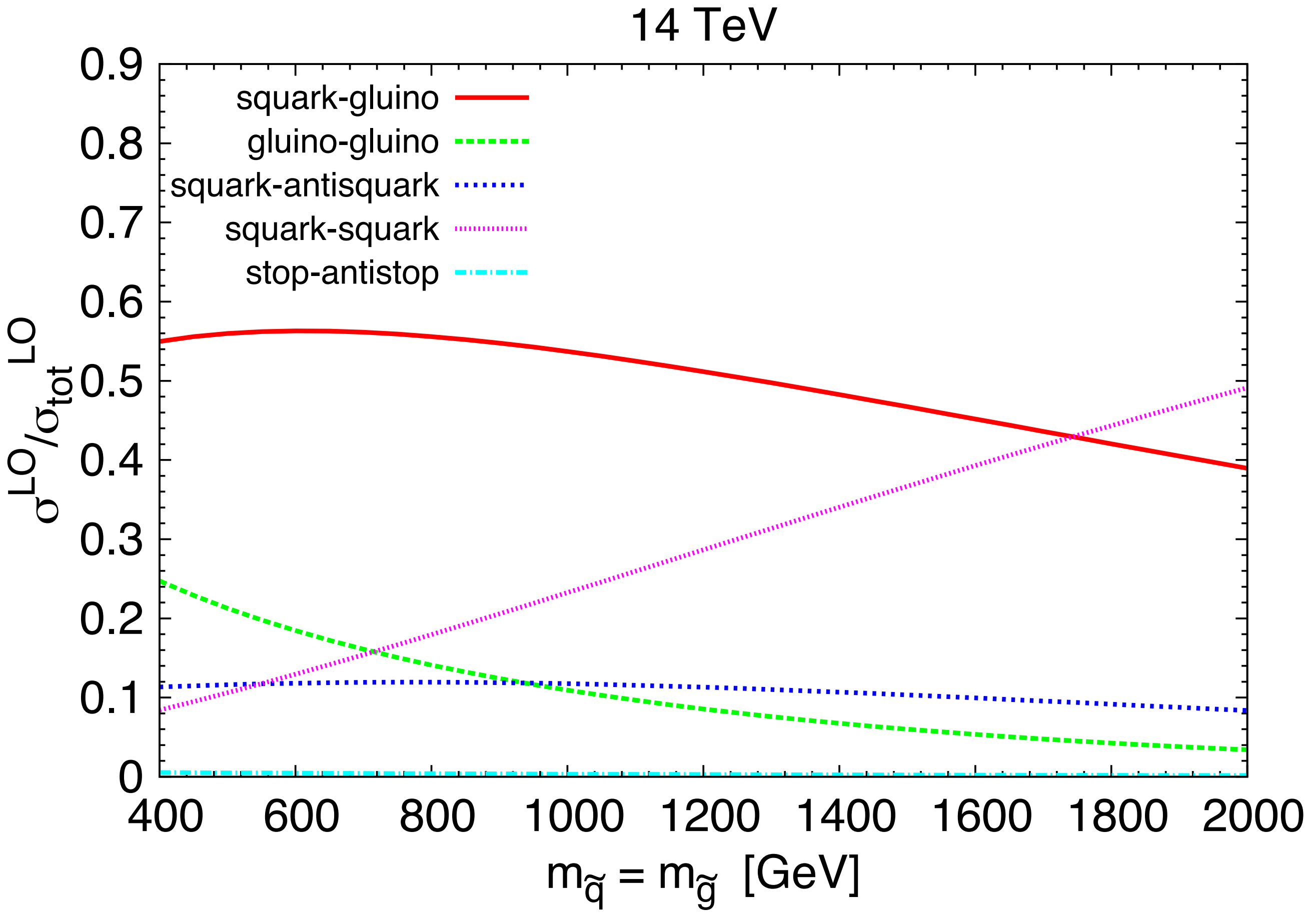

LO in NWA

$$qq' \rightarrow \tilde{q}\tilde{q}' \rightarrow q\tilde{\chi}_1^0 q'\tilde{\chi}_1^0$$

$$\Gamma_{\tilde{q}}/m_{\tilde{q}} \rightarrow 0 \qquad \hat{\sigma}^{(0)}_{\mathrm{NWA}} = \hat{\sigma}^{(0)}(qq' \rightarrow \tilde{q}\tilde{q}') \times BR^{(0)}(\tilde{q} \rightarrow q\tilde{\chi}_1^0) \times BR^{(0)}(\tilde{q}' \rightarrow q'\tilde{\chi}_1^0)$$

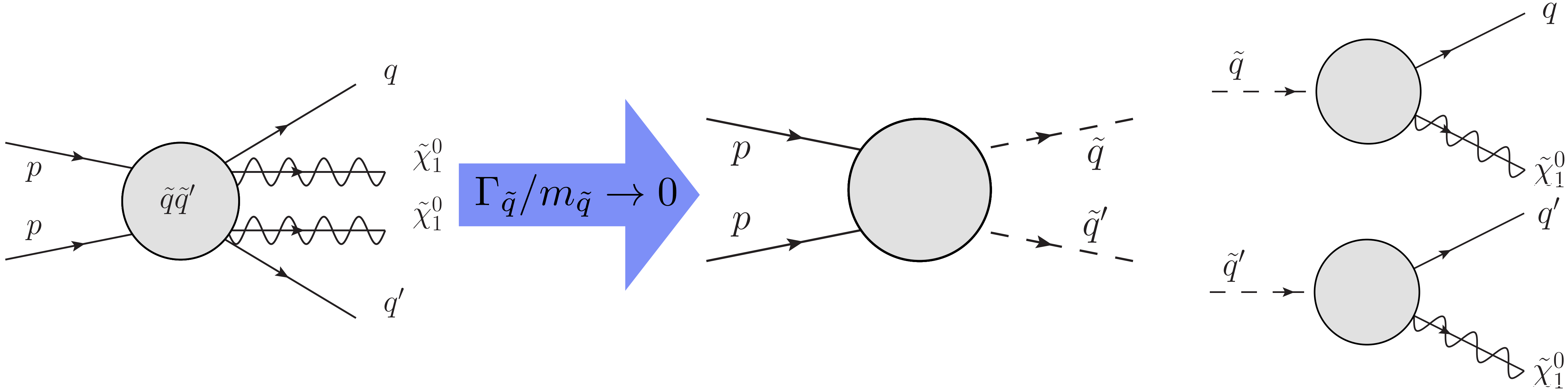

Hadronic differential LO cross section in NWA

$$d\sigma^{(0)}_{\mathrm{NWA}}(pp \rightarrow \tilde{q}\tilde{q}' \rightarrow q\tilde{\chi}_1^0 q'\tilde{\chi}_1^0(+X)) = \frac{1}{\Gamma^{(0)}_{\tilde{q}}\Gamma^{(0)}_{\tilde{q}'}}\left[d\sigma^{(0)}_{pp\rightarrow\tilde{q}\tilde{q}'}\, d\Gamma^{(0)}_{\tilde{q}\rightarrow q\tilde{\chi}_1^0}\, d\Gamma^{(0)}_{\tilde{q}'\rightarrow q'\tilde{\chi}_1^0}\right]$$

NLO in NWA

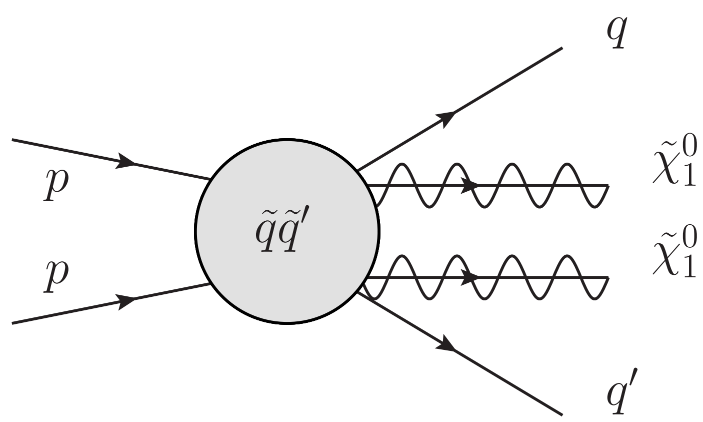

$\Gamma_{\tilde{q}}/m_{\tilde{q}} \to 0$

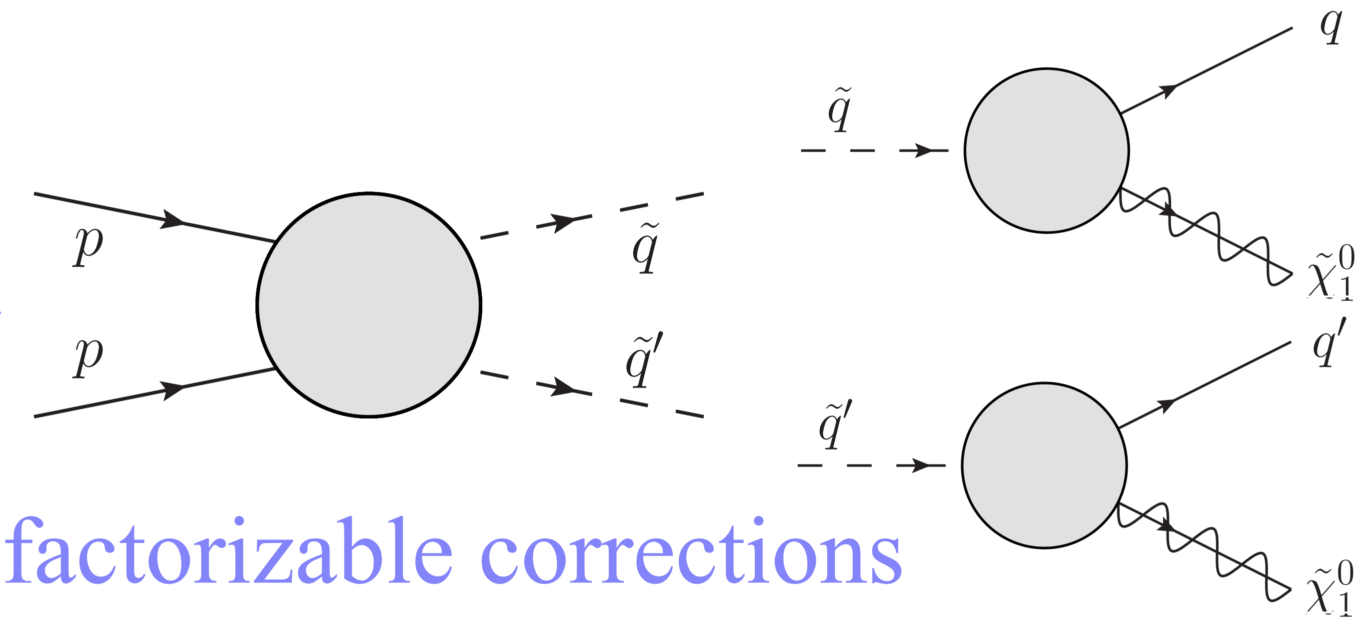

factorizable corrections

Formal expansion in α_s:

Born

$$d\sigma^{(0+1)}_{\text{NWA}}(pp \to \tilde{q}\tilde{q}' \to q\tilde{\chi}_1^0 q'\tilde{\chi}_1^0(+X)) = \frac{1}{\Gamma^{(0)}_{\tilde{q}}\Gamma^{(0)}_{\tilde{q}'}}\Big[d\sigma^{(0)}_{pp\to\tilde{q}\tilde{q}'}\, d\Gamma^{(0)}_{\tilde{q}\to q\tilde{\chi}_1^0}\, d\Gamma^{(0)}_{\tilde{q}'\to q'\tilde{\chi}_1^0}\Big(1 - \frac{\Gamma^{(1)}_{\tilde{q}}}{\Gamma^{(0)}_{\tilde{q}}} - \frac{\Gamma^{(1)}_{\tilde{q}'}}{\Gamma^{(0)}_{\tilde{q}'}}\Big)$$

NLO decay

$$+ d\sigma^{(0)}_{pp\to\tilde{q}\tilde{q}'}\, d\Gamma^{(1)}_{\tilde{q}\to q\tilde{\chi}_1^0}\, d\Gamma^{(0)}_{\tilde{q}'\to q'\tilde{\chi}_1^0} + d\sigma^{(0)}_{pp\to\tilde{q}\tilde{q}'}\, d\Gamma^{(0)}_{\tilde{q}\to q\tilde{\chi}_1^0}\, d\Gamma^{(1)}_{\tilde{q}'\to q'\tilde{\chi}_1^0}$$

NLO production

$$+ d\sigma^{(1)}_{pp\to\tilde{q}\tilde{q}'}\, d\Gamma^{(0)}_{\tilde{q}\to q\tilde{\chi}_1^0}\, d\Gamma^{(0)}_{\tilde{q}'\to q'\tilde{\chi}_1^0}\Big]$$

“master formula”

NLO production

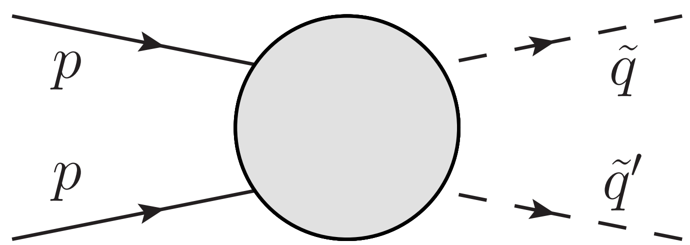

For every chirality and flavour configuration:

$$d\sigma^{(1)}_{pp\to\tilde{q}\tilde{q}'(+X)} = d\sigma^{\text{virtual+soft}}_{pp\to\tilde{q}\tilde{q}'(g)} + d\sigma^{\text{coll}}_{pp\to\tilde{q}\tilde{q}'(g)} + d\sigma^{\text{hard}}_{pp\to\tilde{q}\tilde{q}'g} + d\sigma^{\text{real-quark}}_{pp\to\tilde{q}\tilde{q}'\bar{q}^{(\prime)}}$$

Fully differential cross-section.

NLO decay

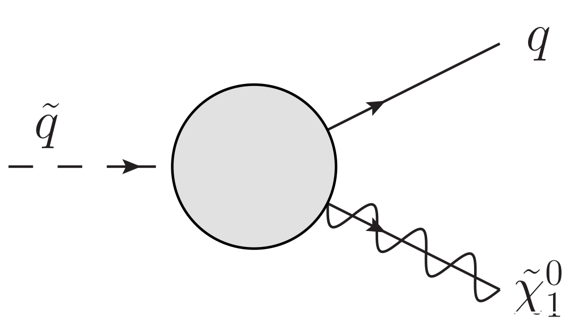

$$d\Gamma^{(1)}_{\tilde{q}\to q\tilde{\chi}^0_1} = d\Gamma^{\text{virtual+soft}}_{\tilde{q}\to q\tilde{\chi}^0_1(g)} + d\Gamma^{\text{coll}}_{\tilde{q}\to q\tilde{\chi}^0_1(g)} + d\Gamma^{\text{hard}}_{\tilde{q}\to q\tilde{\chi}^0_1 g}$$

Fully differential decay.

NLO total decay width

Universal form factor F^{QCD}

$$\Gamma^{(0+1)}_{\tilde{q}\to q\tilde{\chi}^0_j} = \Gamma^{(0)}\left[1 + \frac{4}{3}\frac{\alpha_s}{\pi}F^{QCD}\left(\frac{m_{\tilde{\chi}^0_j}}{m_{\tilde{q}}}, \frac{m_{\tilde{q}}}{m_{\tilde{g}}}\right)\right]$$

$$\sum_{\chi^0_i,\chi^\pm_j}$$

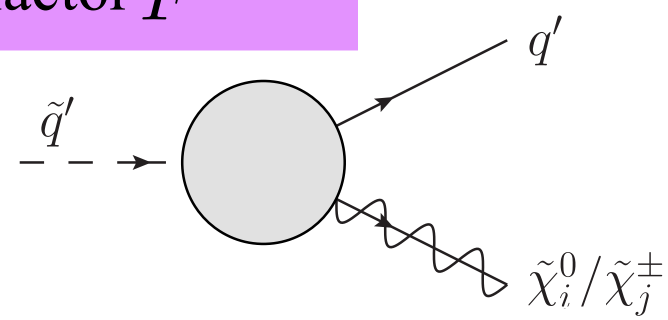

SUSY restoring counterterm

All counterterms, but the one for the QCD coupling $\delta g_s = g_s \delta Z_{g_s}$ are renormalized according to the **on-shell** scheme.

Choice of scheme for the renormalization of the QCD coupling is fixed by definition of α_s in the PDF distributions: $\overline{MS}$ + 5 flavour

$$\delta Z_{g_s} = -\frac{\alpha_s}{4\pi}\left[\Delta\frac{\beta_0}{2} + \frac{1}{3}\log\frac{m_t^2}{\mu_R^2} + \log\frac{m_{\tilde{g}}^2}{\mu_R^2} + \frac{1}{12}\sum_{\tilde{q}}\log\frac{m_{\tilde{q}}^2}{\mu_R^2}\right]$$

Using $\overline{MS}$ and Dim. Reg. breaks supersymmetric Slavnov-Taylor identity, that relates the QCD coupling in the qqg QCD vertex and the $\hat{g}_s$ coupling in the $q\tilde{q}\tilde{g}$ SQCD vertex.

Can be restored:

$$\delta Z_{\hat{g}_s} = \delta Z_{g_s} + \frac{\alpha_s}{3\pi}$$

[Beenakker et al. '96; Hollik, Stöckinger '01]

On-shell subtraction for quark radiation

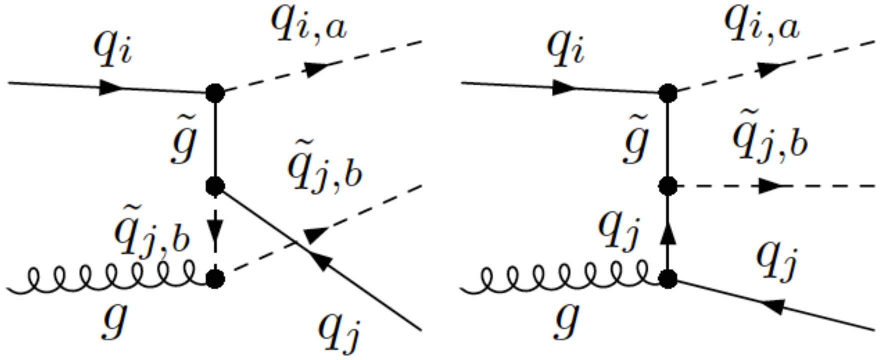

non-resonant

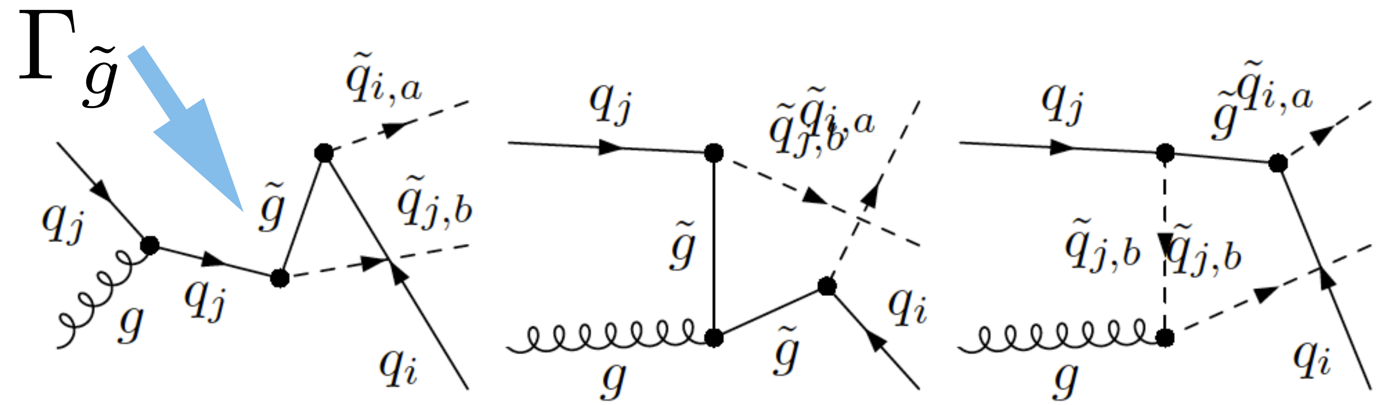

resonant

DR scheme

$$d\hat{\sigma}^{DR}_{q_i g \to \tilde{q}_{ia} \tilde{q}_{ib} \bar{q}_i} \sim \quad d\Pi_{(2\to 3)} \left[\overline{|\mathcal{M}_{\text{nonres}}|^2} + 2\text{Re}\overline{(\mathcal{M}_{\text{nonres}} \mathcal{M}^*_{\text{res}})} \right]$$

DS scheme

$$d\hat{\sigma}^{DS}_{q_i g \to \tilde{q}_{ia} \tilde{q}_{ib} \bar{q}_i} \sim \quad \left[\overline{|\mathcal{M}_{\text{nonres}}|^2} + 2\text{Re}\overline{(\mathcal{M}_{\text{nonres}} \mathcal{M}^*_{\text{res}})} + \overline{|\mathcal{M}_{\text{res}}|^2} \right] d\Pi_{(2\to 3)} - \left[\overline{|\mathcal{M}_{\text{res},1}|^2} + \overline{|\mathcal{M}_{\text{res},2}|^2} \right] d\Pi_{(2\to 2)\times(1\to 2)} \; .$$

and numerically: $\Gamma \to 0$

Numerical results

For **SPS1a (14 TeV)**: Scale variation: $\boldsymbol{\mu_f = \mu_r = (m/2, m, 2m)}$, m: average $\tilde{q}$ mass

SPS1a	$\tilde{u}_L$	$\tilde{u}_R$	$\tilde{d}_L$	$\tilde{d}_R$	$\tilde{g}$	$\tilde{\chi}_1^0$
mass (GeV)	563.6	546.7	569.0	546.6	608.5	97.0

(PDFs: CTEQ6.6 both for LO and NLO)

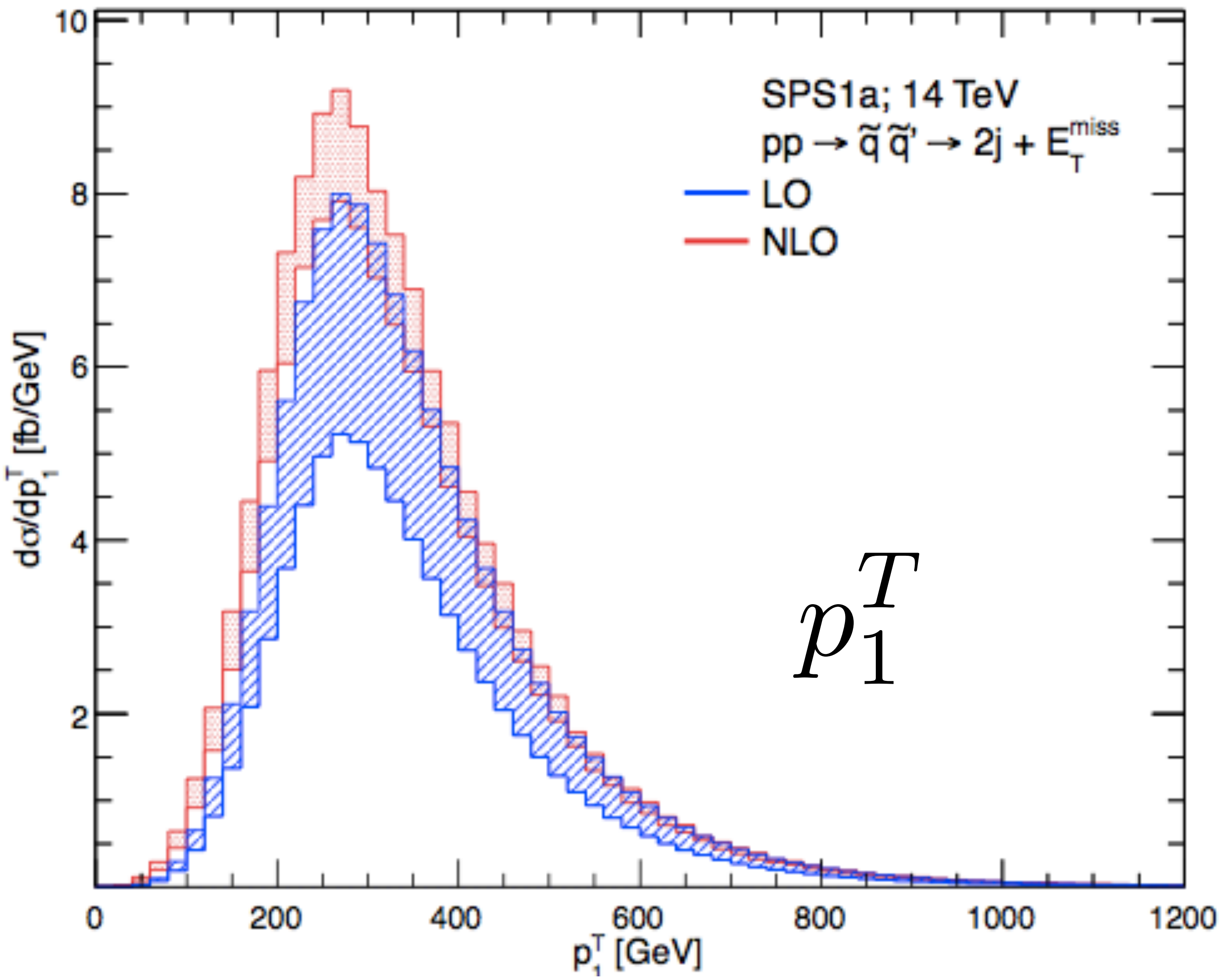

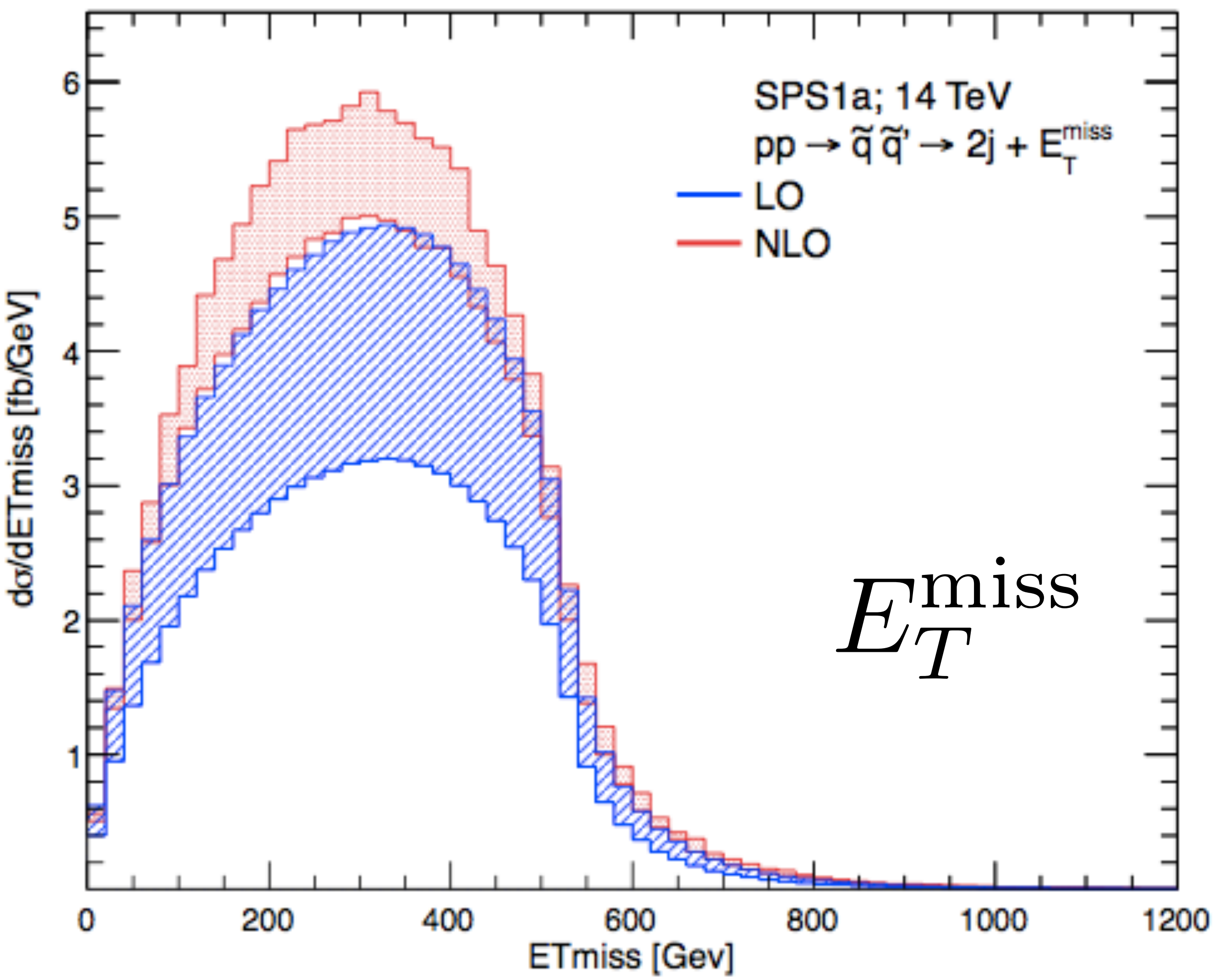

On-shell subtraction

DR vs. DS

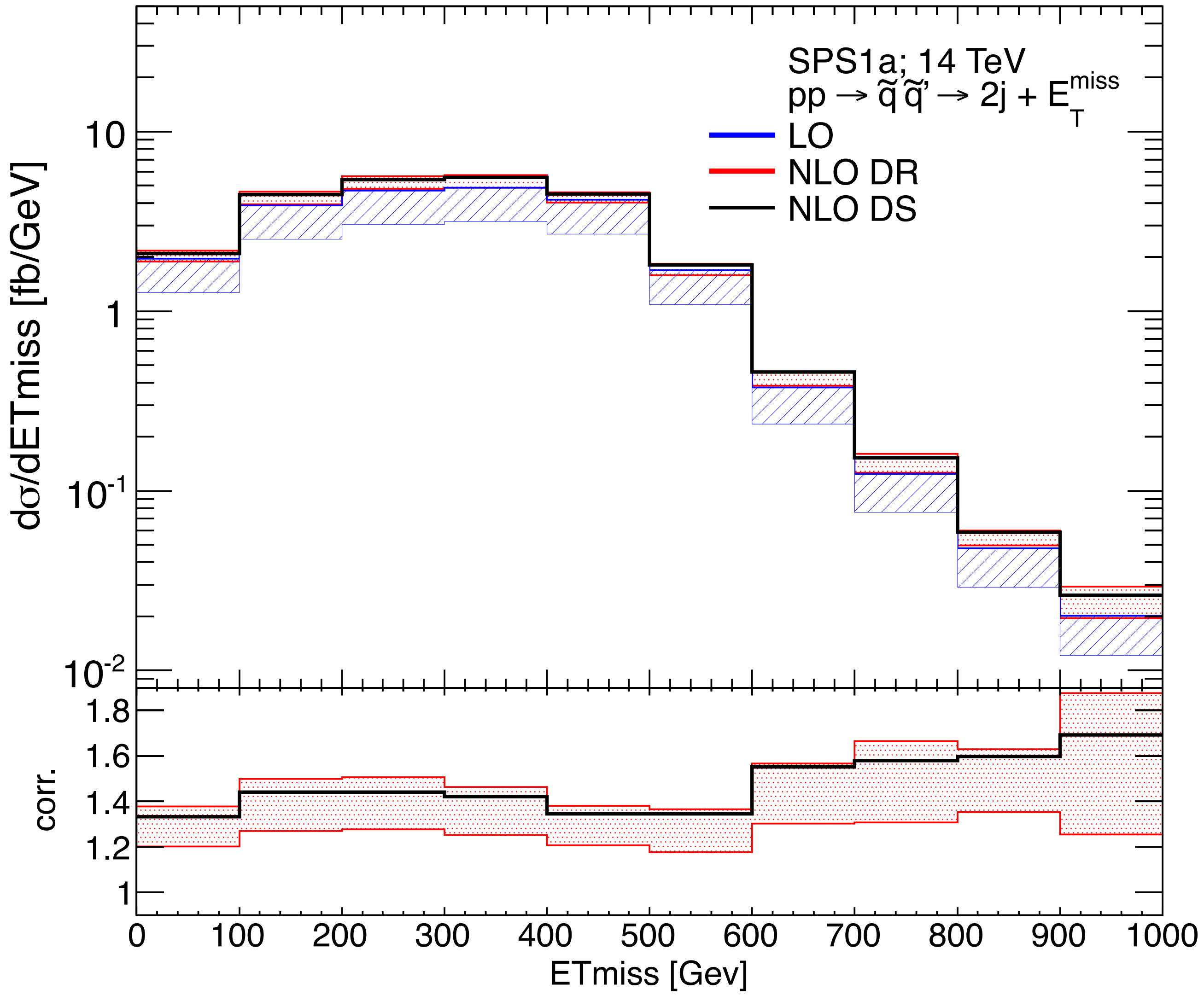

$$E_T^{\text{miss}}$$

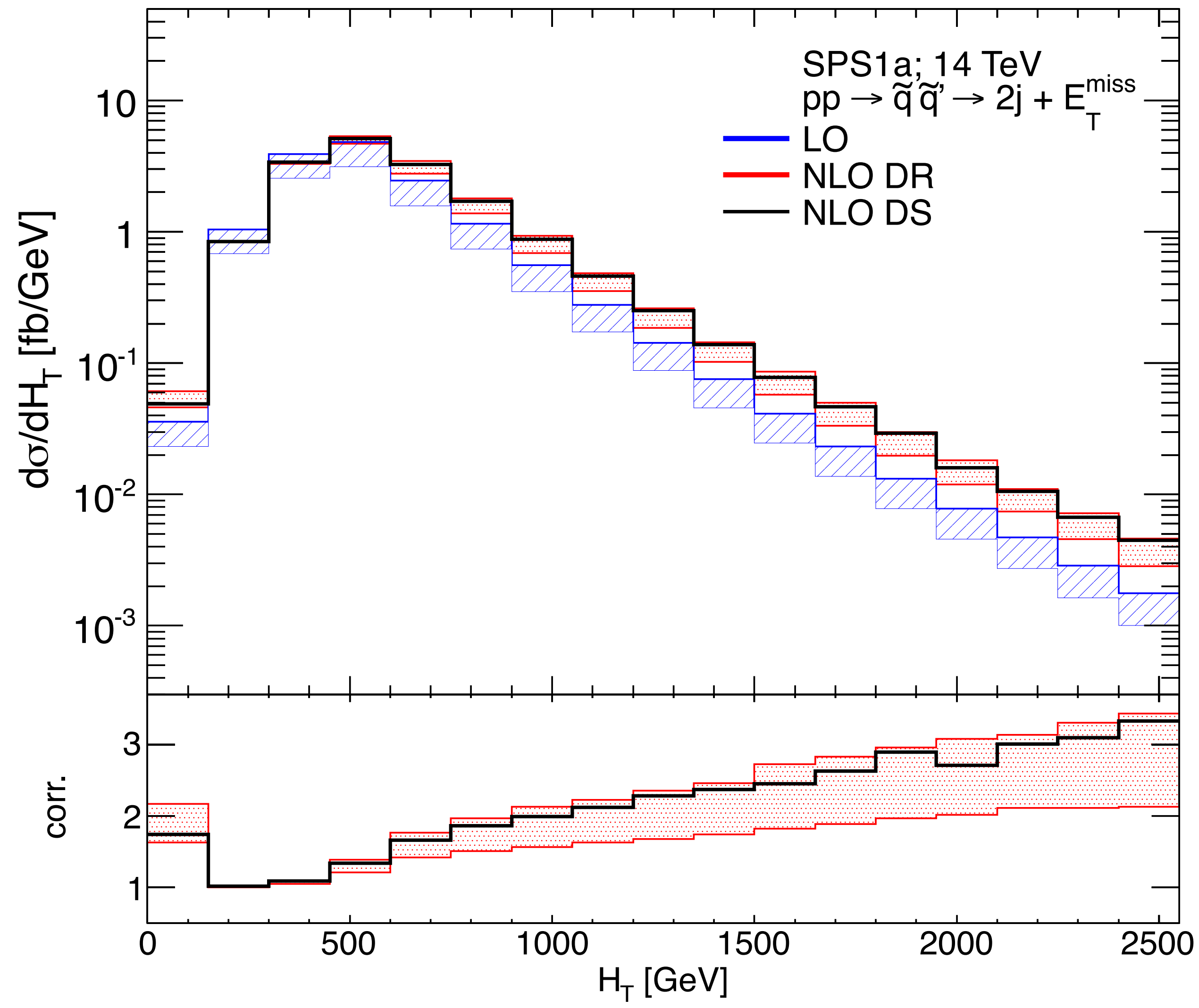

$$H_T = \sum_{i=1,2(,3)} p_i^{\mathrm{T}}$$

CMSSM 10.1.5 (14 TeV)

Comparison between NLO and LO rescaled by global K-factor: corrections purely in the **shapes**

10.1.5	$\tilde{u}_L$	$\tilde{u}_R$	$\tilde{d}_L$	$\tilde{d}_R$	$\tilde{g}$	$\tilde{\chi}_1^0$
mass (GeV)	1437.7	1382.3	1439.7	1376.9	1568.6	291.3

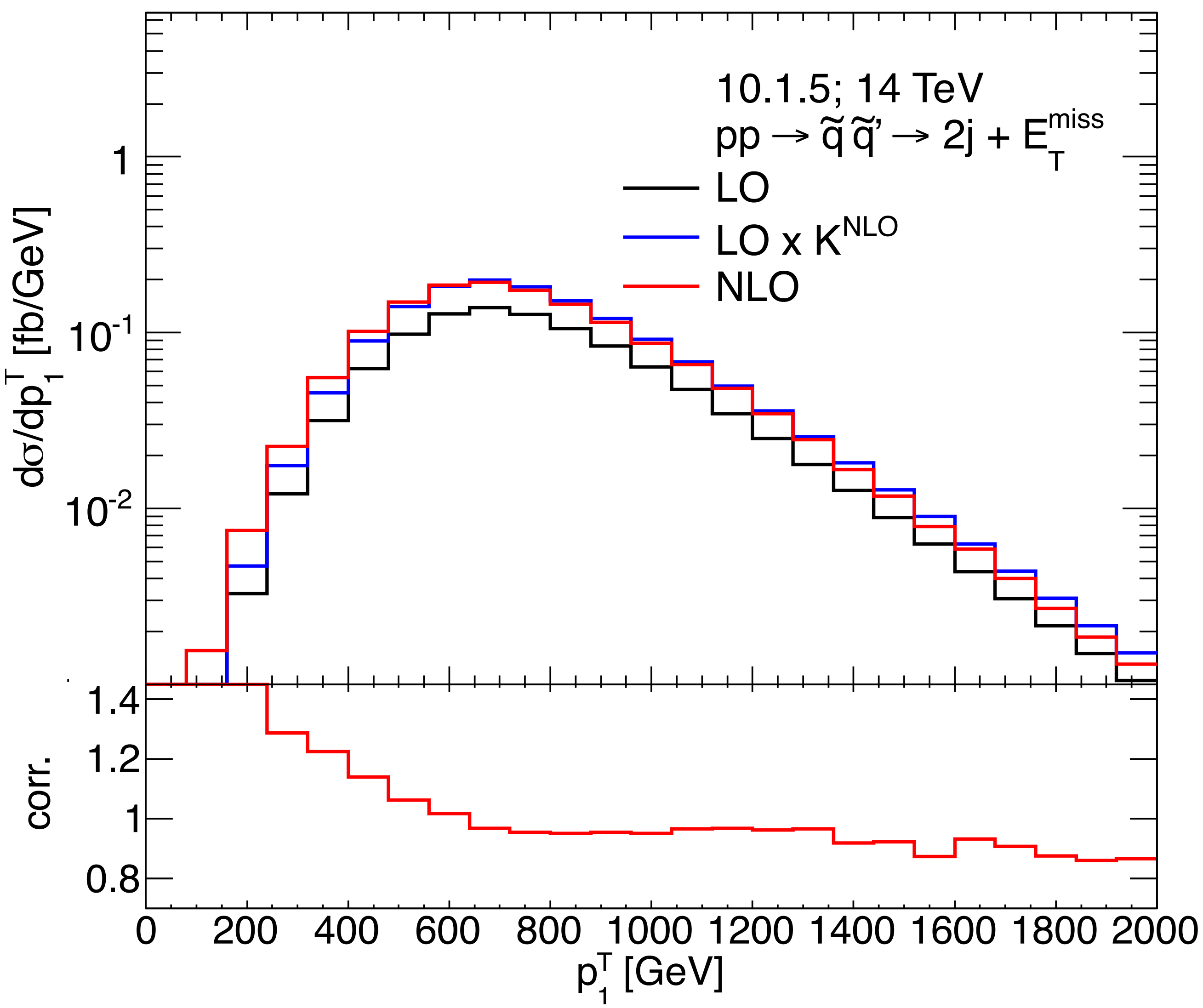

p_1^T

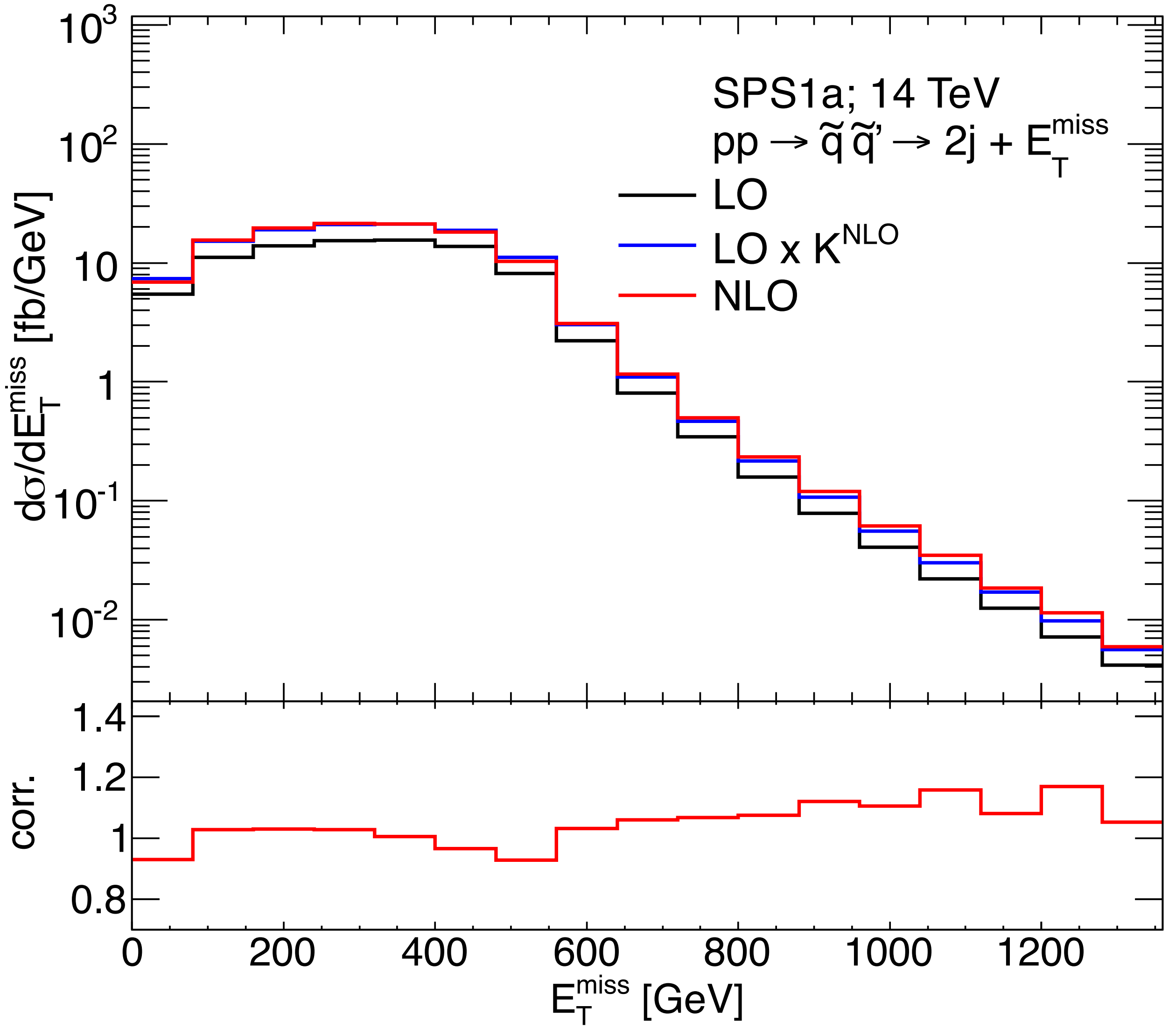

E_T^{miss}

CMSSM 10.1.5 (14 TeV)
Comparison between NLO and LO rescaled by global K-factor: corrections purely in the **shapes**

10.1.5	$\tilde{u}_L$	$\tilde{u}_R$	$\tilde{d}_L$	$\tilde{d}_R$	$\tilde{g}$	$\tilde{\chi}_1^0$
mass (GeV)	1437.7	1382.3	1439.7	1376.9	1568.6	291.3

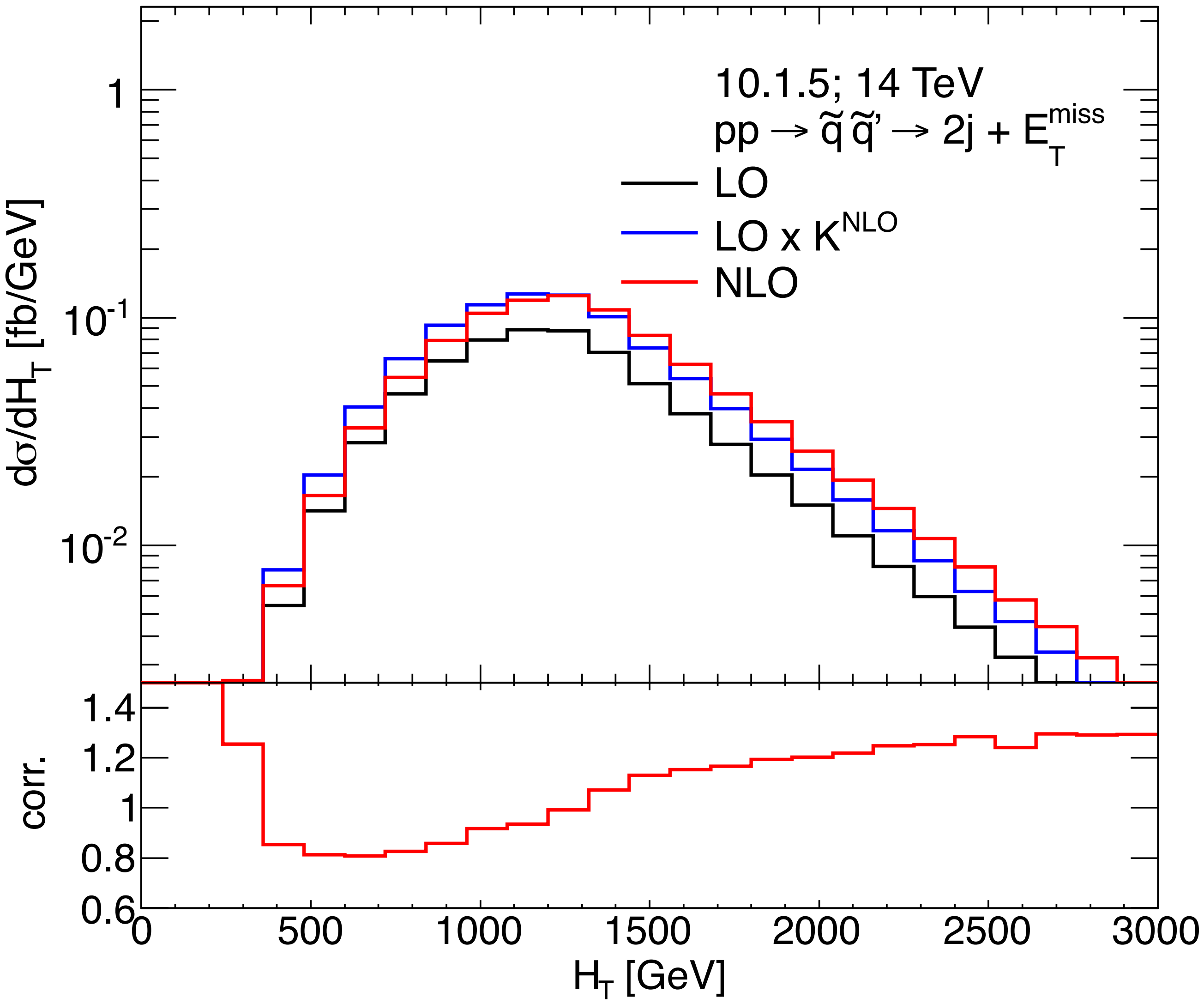

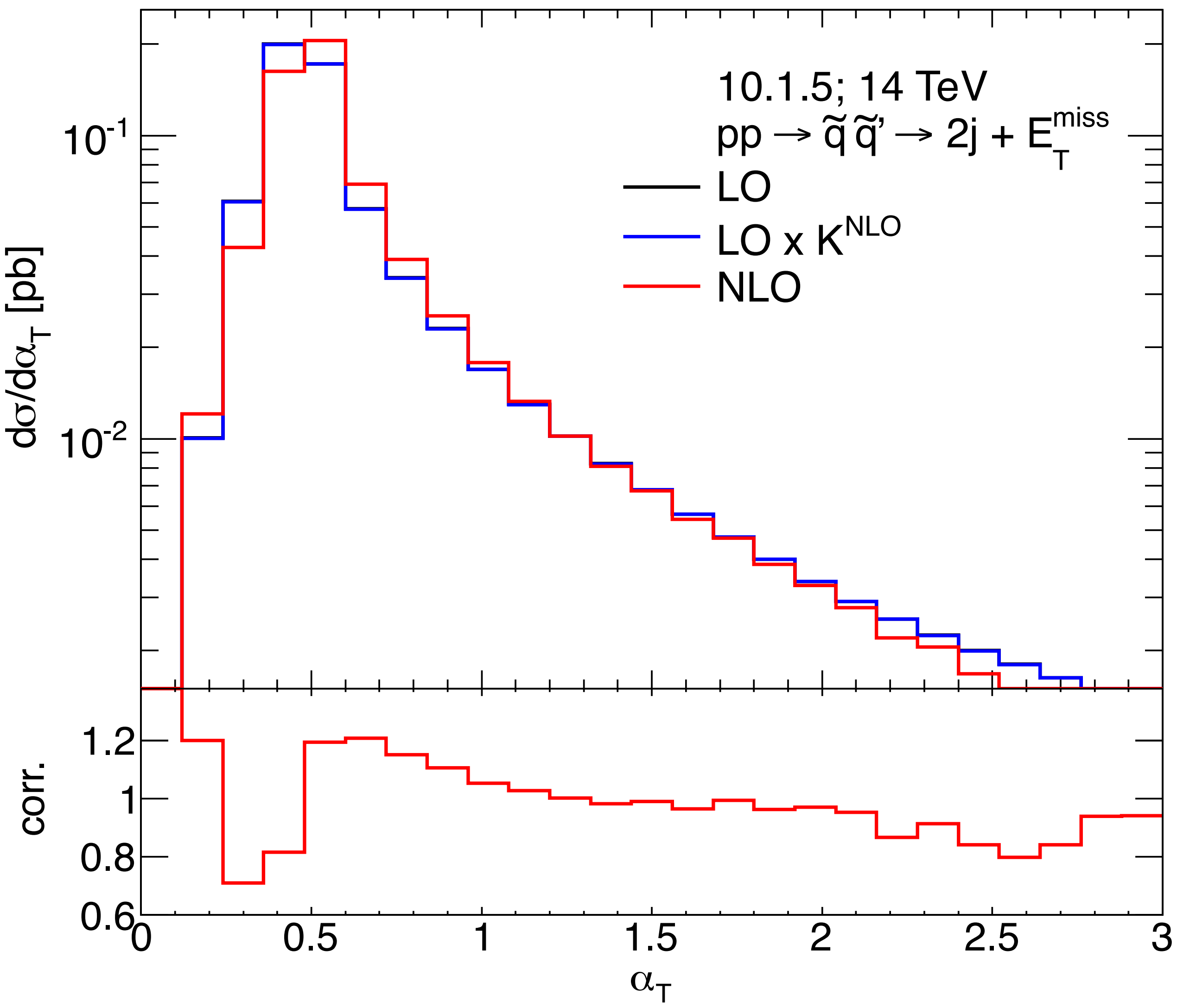

$$H_T = \sum_{i=1,2(,3)} p_i^{\mathrm{T}}$$

$$\alpha_{\mathrm{T}} = E_{\mathrm{T}}^{j_2} / M_{\mathrm{T}}$$

CMSSM 10.1.5 (14 TeV)
Comparison between NLO and LO rescaled by global K-factor:
corrections purely in the **shapes**

10.1.5	$\tilde{u}_L$	$\tilde{u}_R$	$\tilde{d}_L$	$\tilde{d}_R$	$\tilde{g}$	$\tilde{\chi}_1^0$
mass (GeV)	1437.7	1382.3	1439.7	1376.9	1568.6	291.3

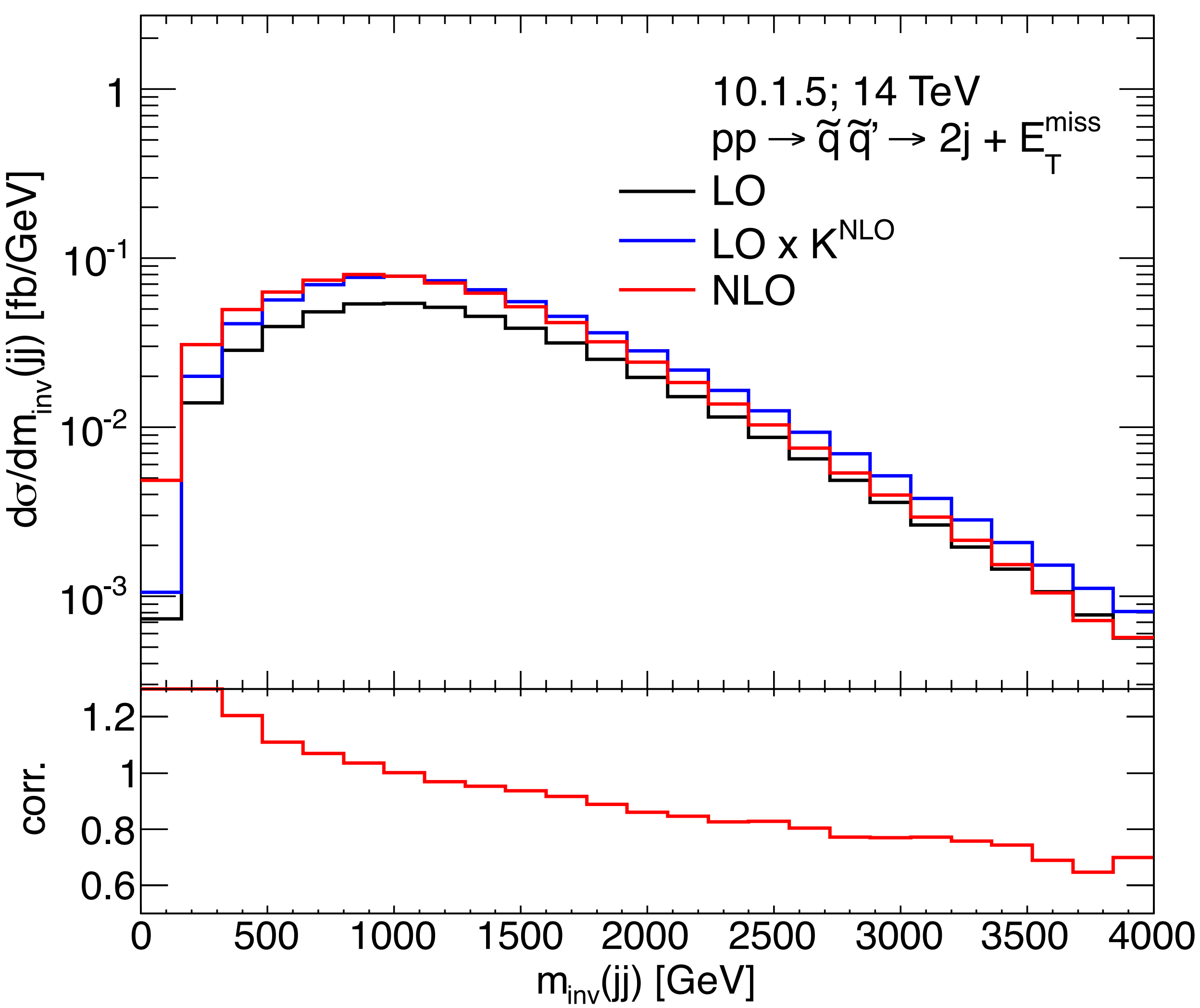

$$m_{\text{inv}}(jj)$$

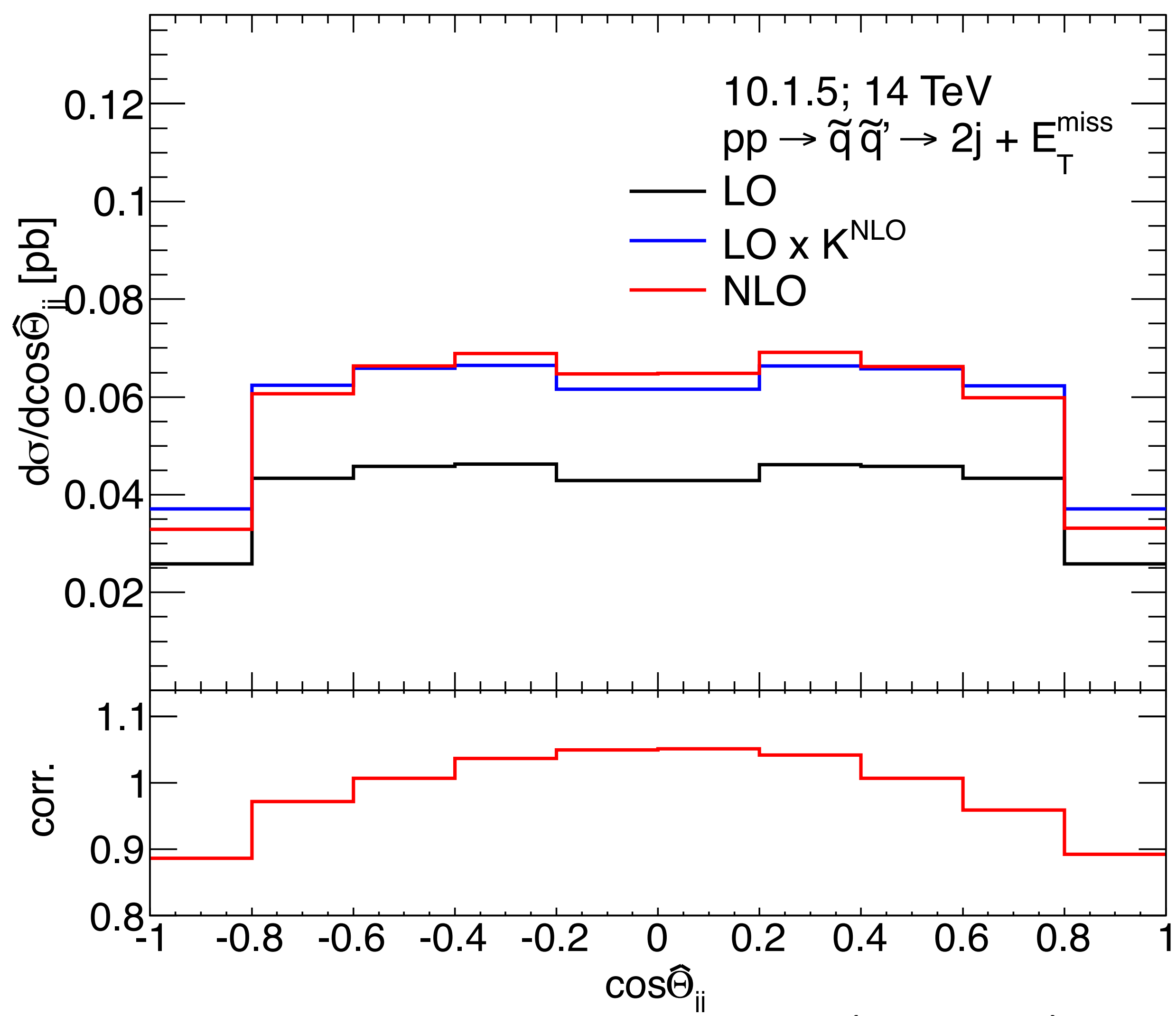

$$\cos\hat{\Theta} = \tanh\left(\frac{\Delta\eta_{jj}}{2}\right)$$

Effect on cut-and-count searches performed by **ATLAS** in 2j -signal region:

$$p^{\mathrm{T}}_{j_1} > 130\ \mathrm{GeV},\ p^{\mathrm{T}}_{j_2} > 40\ \mathrm{GeV},\ |\eta_{j_{1/2}}| < 2.8,\ \Delta\phi(j_{1/2}, \vec{\not{E}}_T) > 0.4$$

$$m_{\mathrm{eff}} > 1\ \mathrm{TeV},\ \not{E}_T/m_{\mathrm{eff}} > 0.3,$$

differential combined NLO

benchmarkpoint	**Energy [TeV]**	$N^{(0)}_{\mathrm{ATLAS}}$	$N^{(0+1)}_{\mathrm{ATLAS}}$	$K_{N_{\mathrm{ATLAS}}}$	$K_{pp\to\tilde{q}\tilde{q}'}$
SPS1a	7	0.066 pb	0.083 pb	1.26	1.37
	8	0.097 pb	0.121 pb	1.25	1.35
	14	0.347 pb	0.424 pb	1.22	1.28
10.1.5	7	0.313 fb	0.503 fb	1.61	1.57
	8	0.861 fb	1.344 fb	1.56	1.52
	14	13.82 fb	19.77 fb	1.43	1.40

flat K-factor of just production

Effect on cut-and-count searches performed by **CMS** in α_T-signal region:

$$p^{\mathrm{T}}_{j_{1/2}} > 100\ \mathrm{GeV},\ |\eta_{j_1}| < 2.5,\ |\eta_{j_2}| < 3.0,$$

$$H_T > 350\ \mathrm{GeV},\ \not{H}_T/\not{E}_T < 1.25,\ \alpha_T > 0.55,$$

benchmarkpoint	**Energy [TeV]**	$N^{(0)}_{\mathrm{CMS}}$	$N^{(0+1)}_{\mathrm{CMS}}$	$K_{N_{\mathrm{CMS}}}$	$K_{pp\to\tilde{q}\tilde{q}'}$
SPS1a	7	0.112 pb	0.141 pb	1.26	1.37
	8	0.157 pb	0.197 pb	1.25	1.35
	14	0.488 pb	0.614 pb	1.26	1.28
10.1.5	7	0.201 pb	0.261 pb	1.30	1.57
	8	0.542 fb	0.674 fb	1.24	1.52
	14	8.129 fb	8.884 fb	1.09	1.40

Combining production and a decay chain at NLO

We study the experimental signature

$$2j + 2l + \not{E}_T (+X)$$

via squark-squark production and an attached EW decay chain.

$$pp \to \tilde{q}_L \tilde{q}'_R \to q \tilde{\chi}^0_1 q' l^+ l^- \tilde{\chi}^0_1 (+X)$$

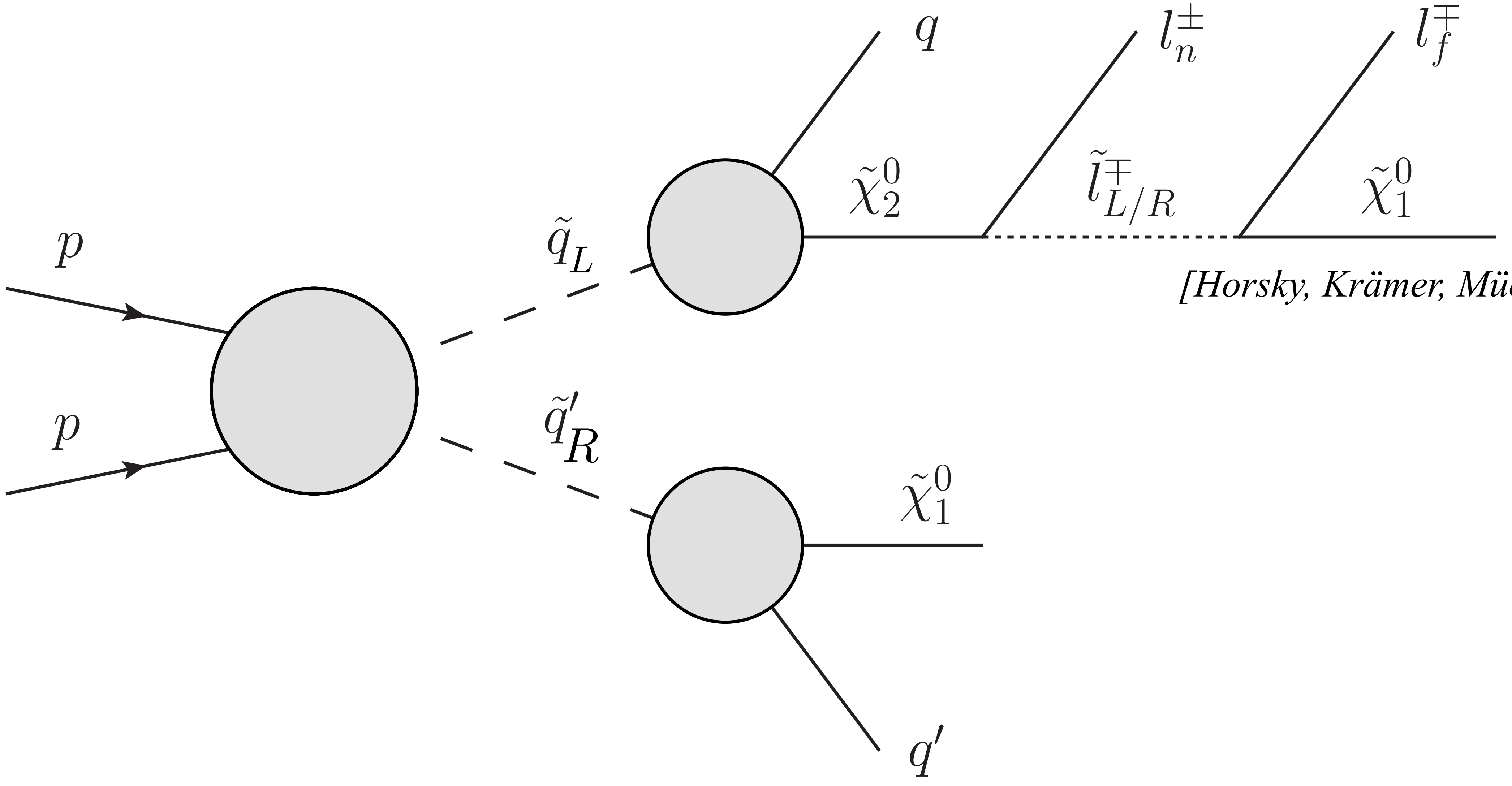

[Horsky, Krämer, Mück, Zerwas '08]

The “golden” decay chain

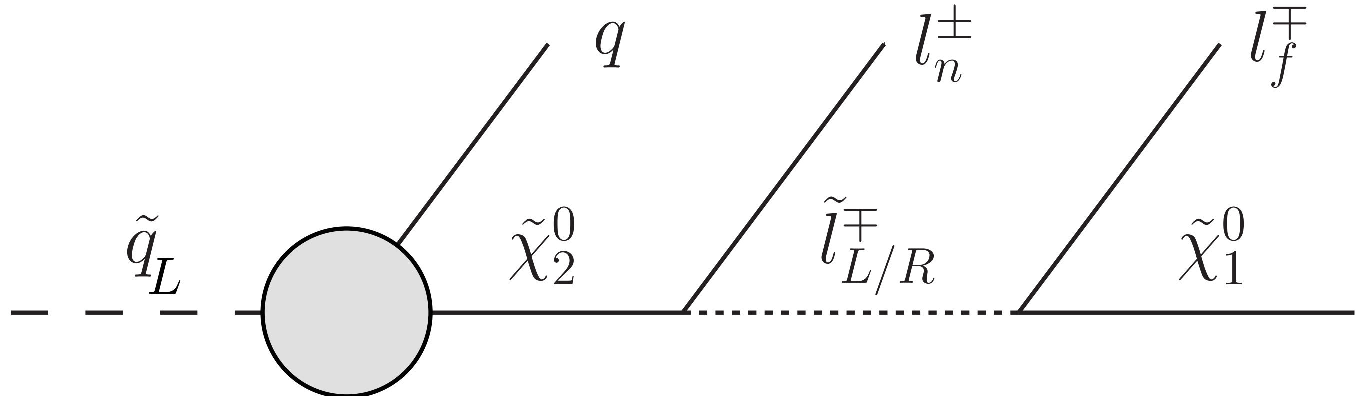

- Search for SUSY in “jets + OSSF leptons” channel
- Possible to measure **masses** of intermediate sparticles from invariant mass distribution endpoints and shapes (m_{jll}, $m_{jl(high)}$, $m_{jl(low)}$,...).
- Possible to measure **spin** of sparticles via charge asymmetries.

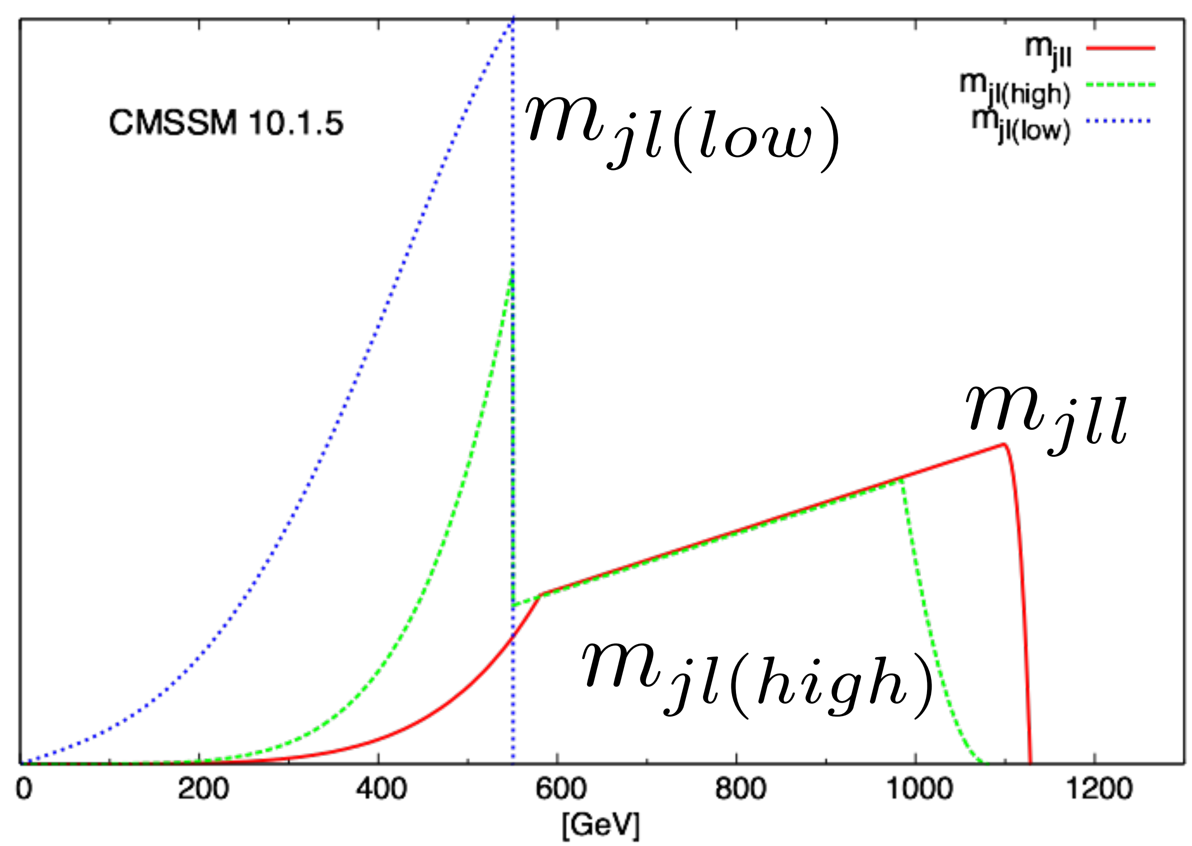

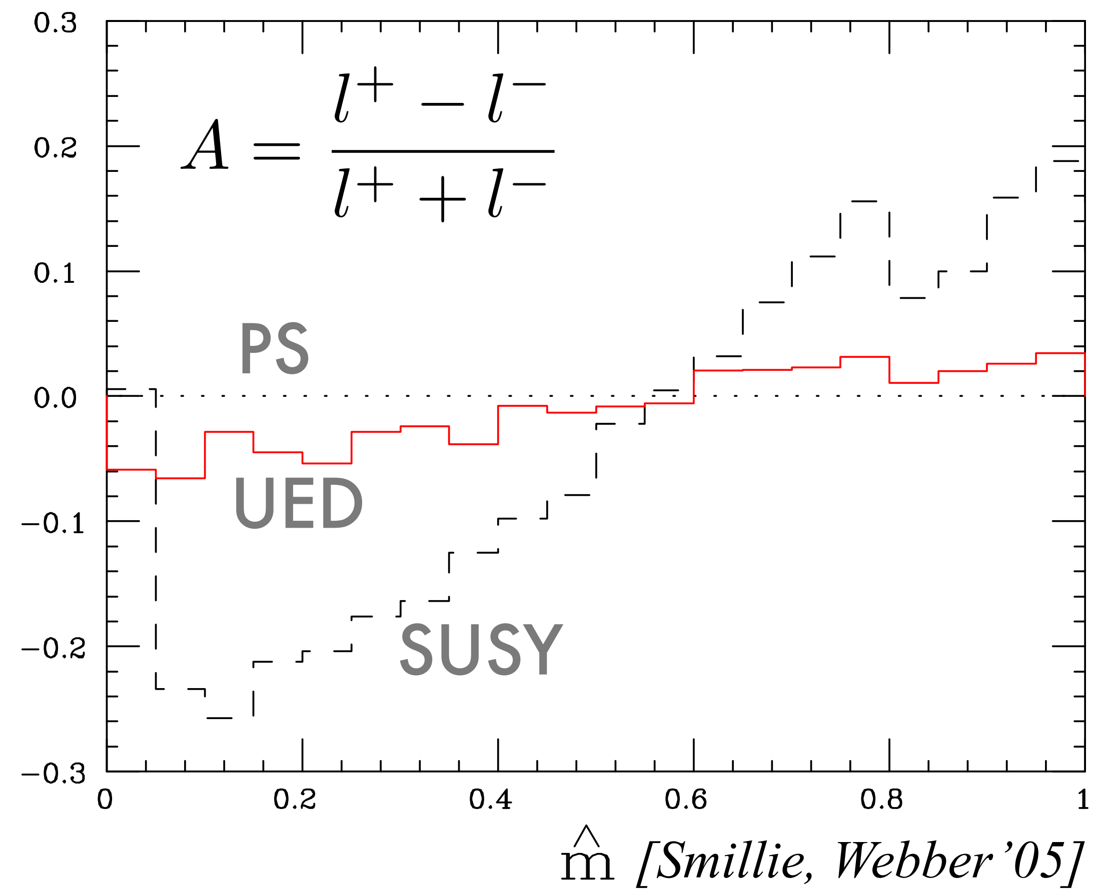

[Smillie, Webber’05]

Comparison between NLO and LO corrections purely in the **shapes** of distributions.

10.1.5	$\tilde{u}_L$	$\tilde{u}_R$	$\tilde{d}_L$	$\tilde{d}_R$	$\tilde{g}$	$\tilde{\chi}_1^0$
mass (GeV)	1437.7	1382.3	1439.7	1376.9	1568.6	291.3

LHC 14 TeV

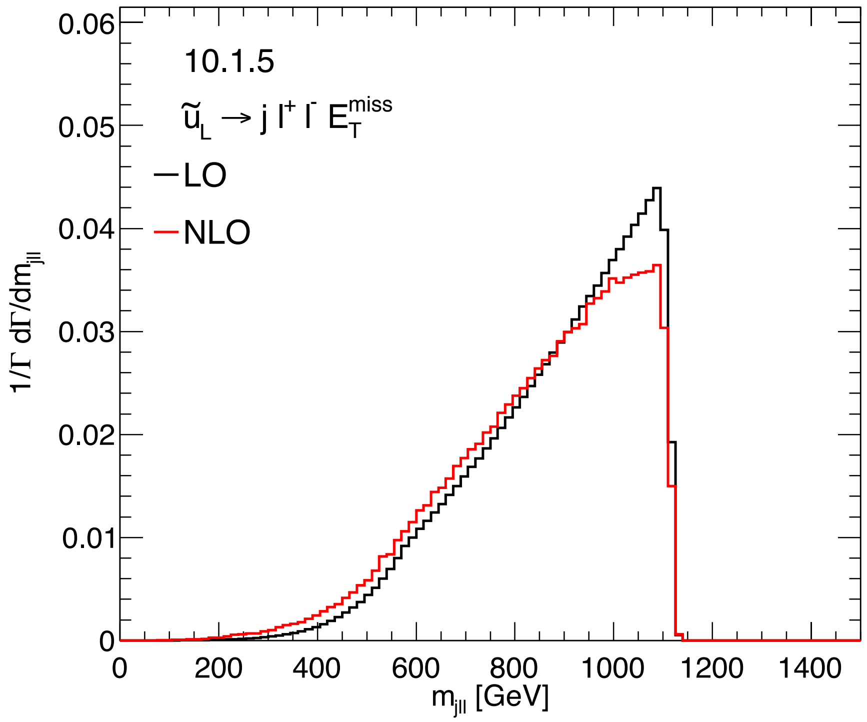

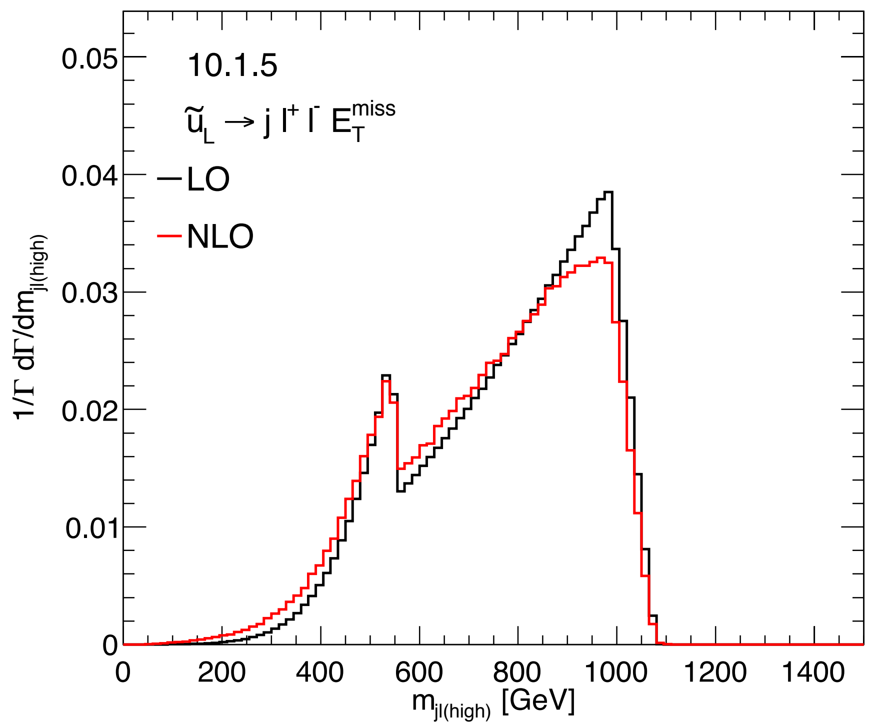

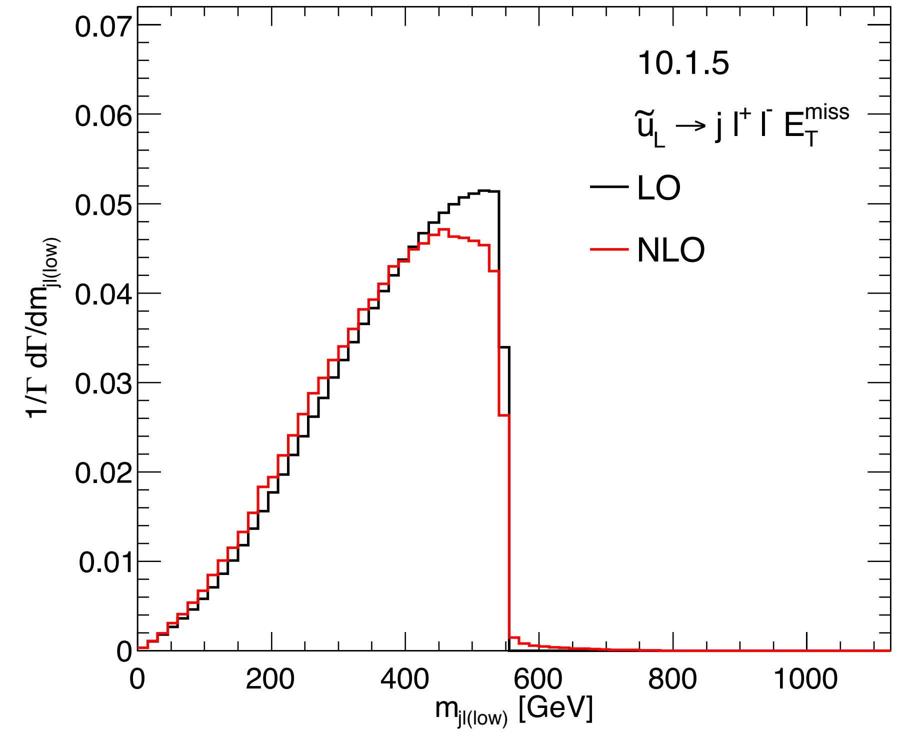

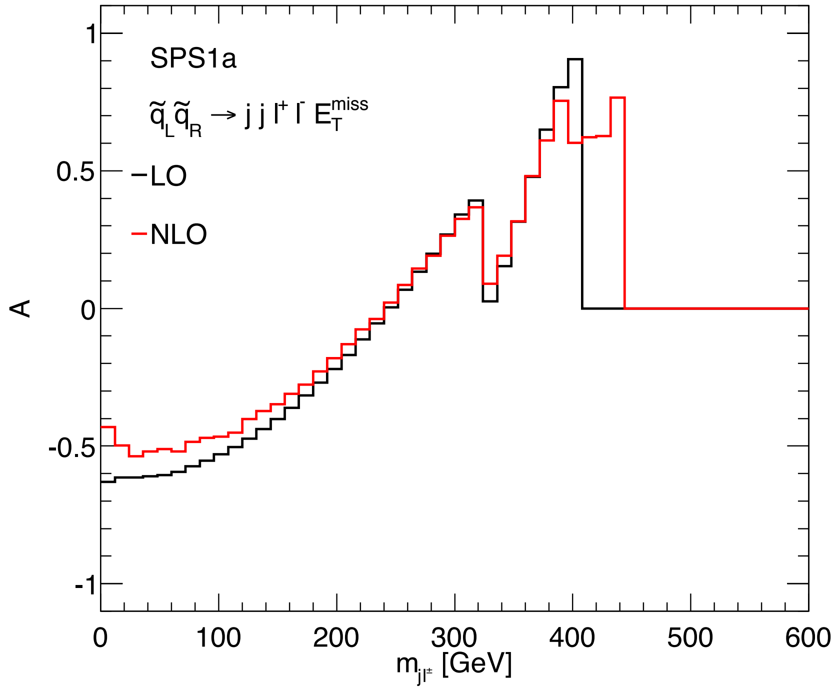

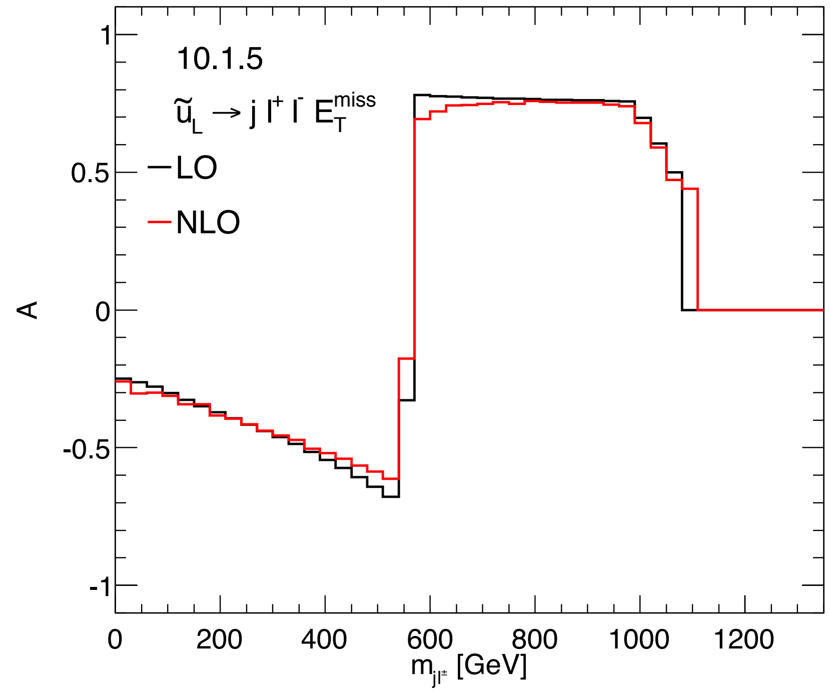

Conclusion

Knowledge of higher-order corrections to squark/gluino processes are important for precise description of physical observables and thus for setting **accurate limits** and even more for **parameter determination**.

We provide a fully differential calculation of factorizable NLO QCD corrections in NWA for squark-squark production and different decays.

Using a flat K-factor is not always a reliable approximation.

Outlook

Study of further experimental signatures and non-factorizable corrections.

Fully differential NLO QCD predictions of combined production and decay for all squark/gluino channels are desirable (matched to a NLO PS).

(Hopefully) discovery of SUSY in the next run of the LHC.

p19MSSM1A (14 TeV)
Comparison between NLO and LO rescaled by global K-factor:
corrections purely in the **shapes**

p19MSSM1	$\tilde{u}_L$	$\tilde{u}_R$	$\tilde{d}_L$	$\tilde{d}_R$	$\tilde{g}$	$\tilde{\chi}_1^0$
mass (GeV)	339.6	394.8	348.3	392.7	414.7	299.1

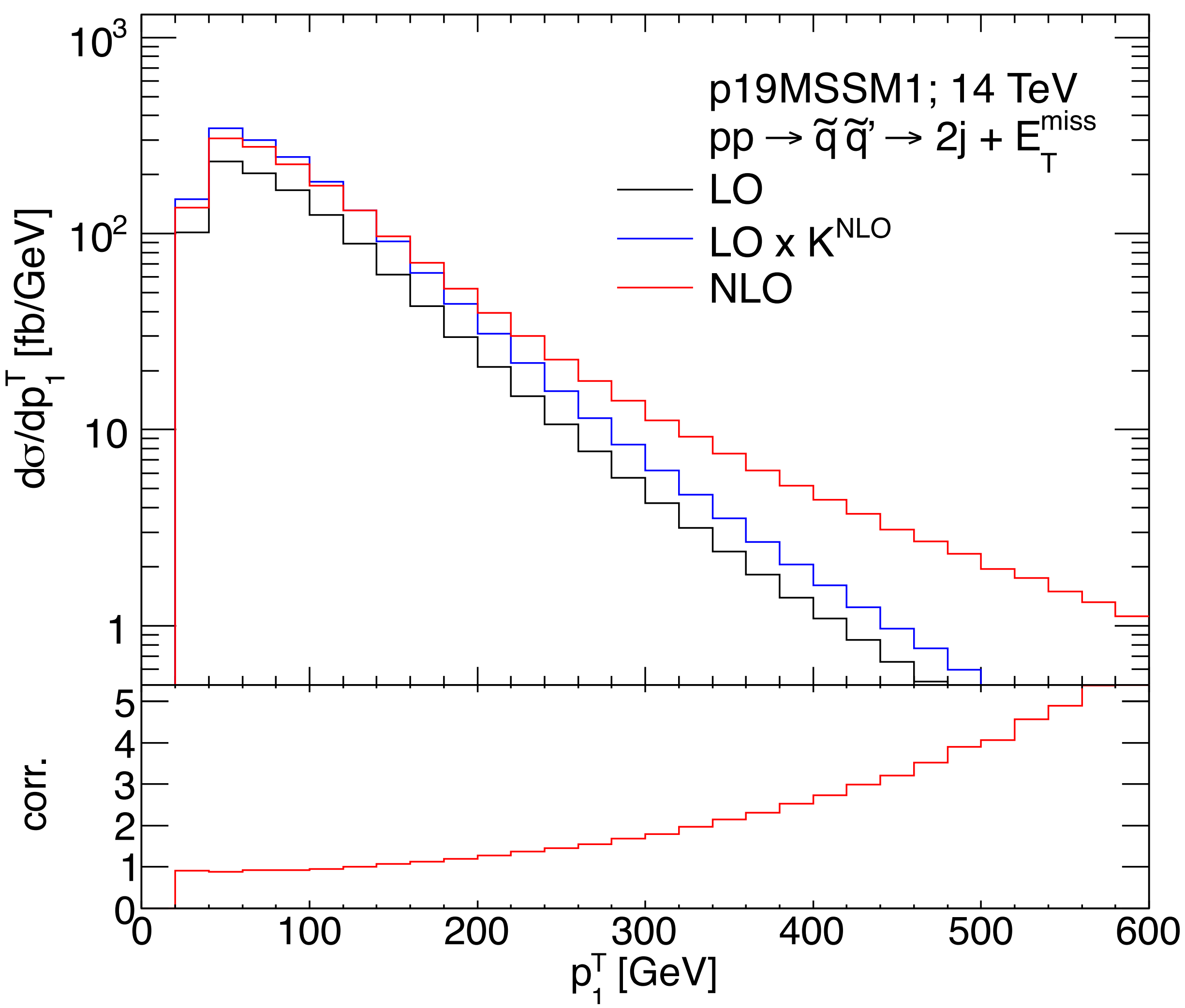

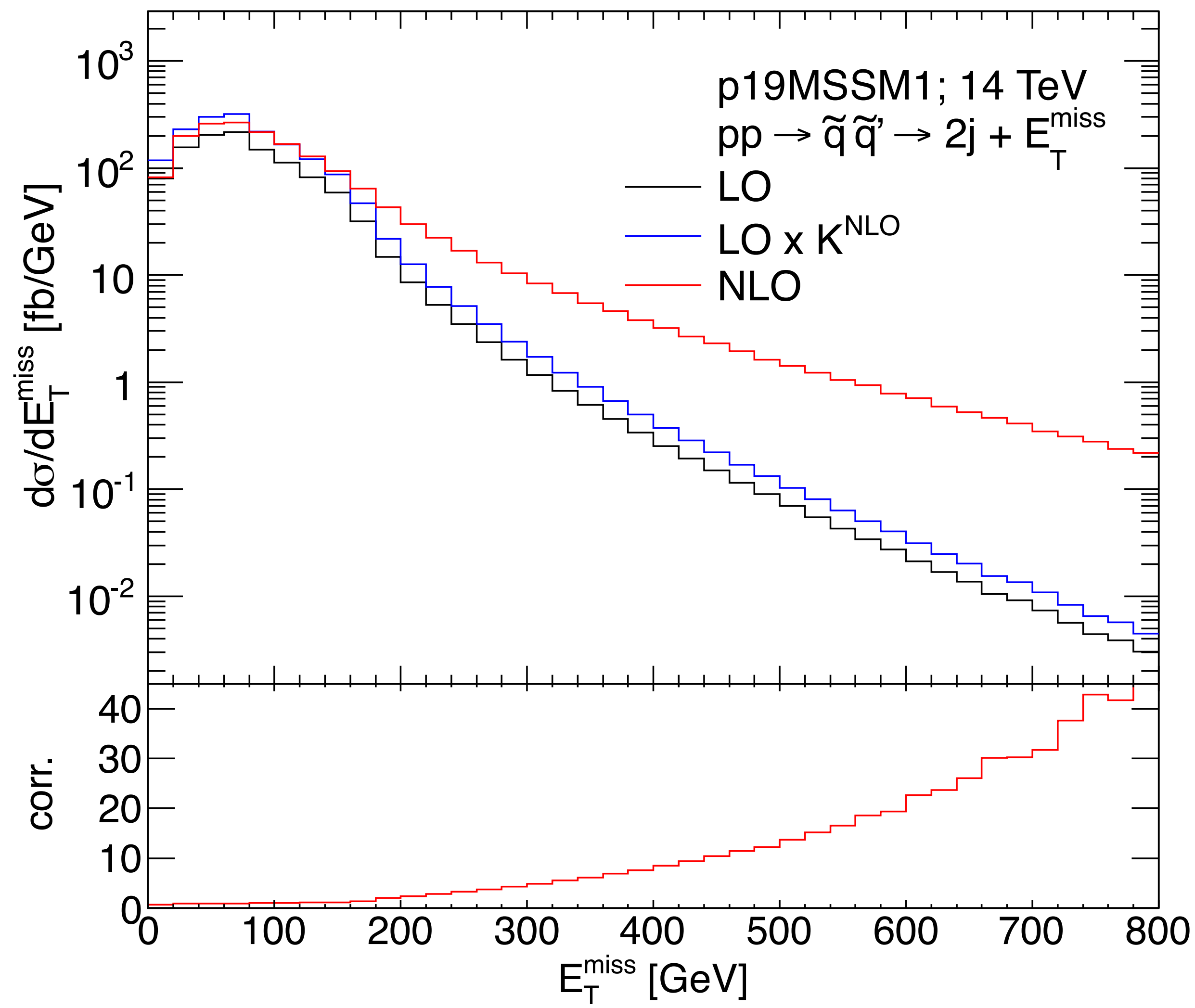

p_1^T see also: Plehn, Rainwater, Skands '07; Alwall, de Visscher, Maltoni '08 $E_T^{\rm miss}$

NLO production

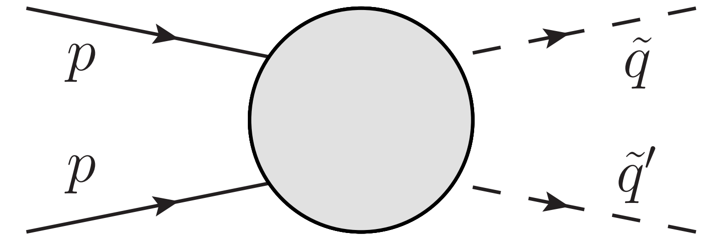

$$d\sigma^{(1)}_{pp\to\tilde{q}\tilde{q}'(+X)} = d\sigma^{\text{virtual+soft}}_{pp\to\tilde{q}\tilde{q}'(g)} + d\sigma^{\text{coll}}_{pp\to\tilde{q}\tilde{q}'(g)} + d\sigma^{\text{hard}}_{pp\to\tilde{q}\tilde{q}'g} + d\sigma^{\text{real-quark}}_{pp\to\tilde{q}\tilde{q}'\bar{q}^{(\prime)}}$$

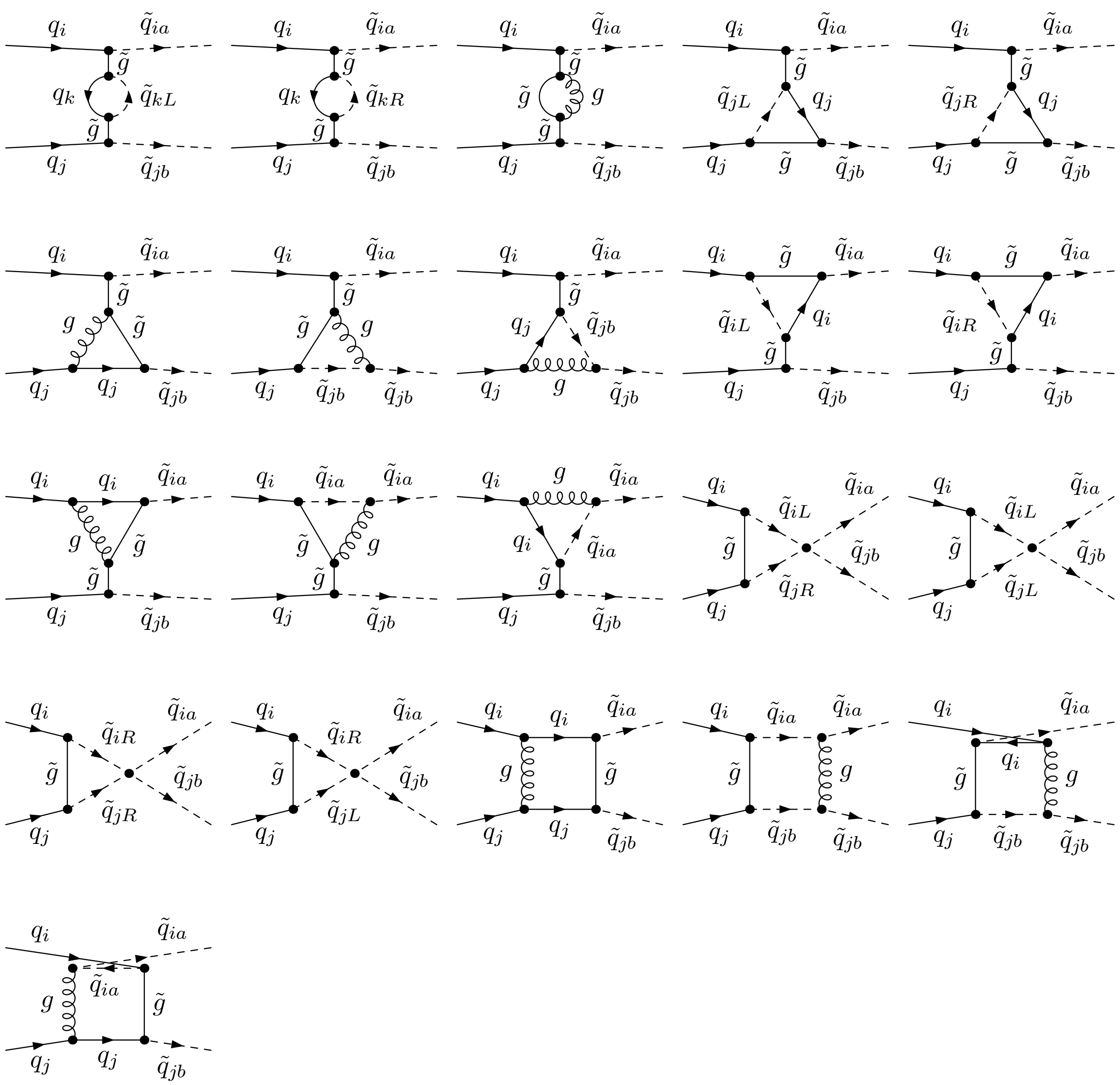

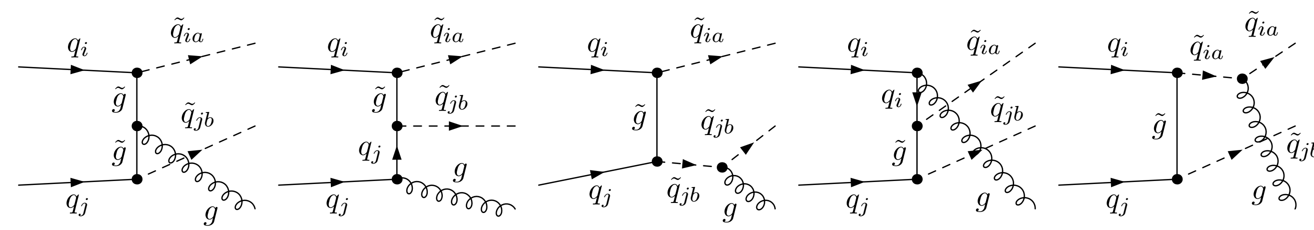

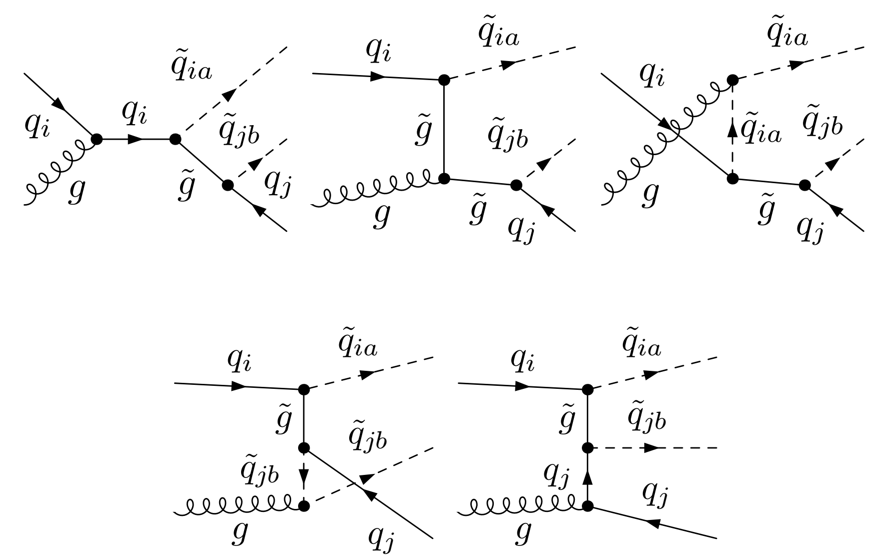

On-shell subtraction

DR vs DS

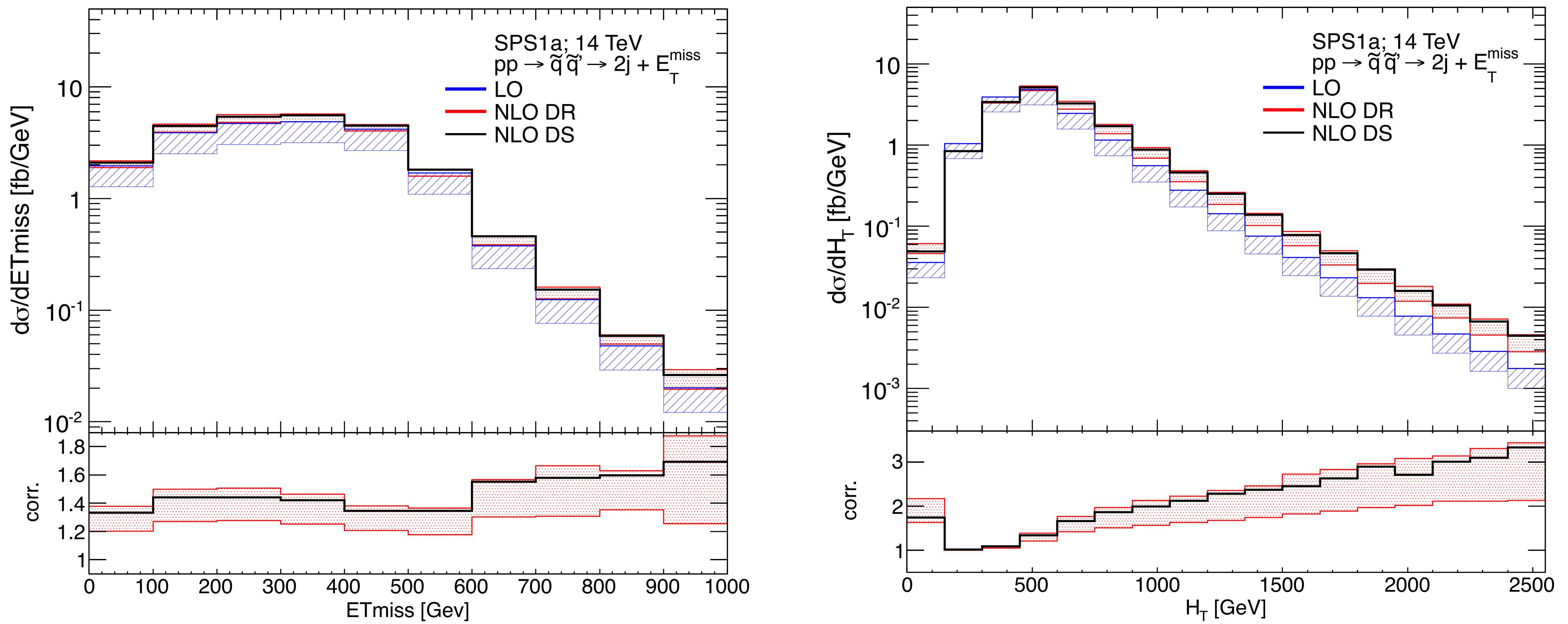

global vs. local DS

benchmark	$\sqrt{S}$ [TeV]	$\sigma^{(0)}_{pp\to\tilde{q}\tilde{q}'}$	$K^{DR}_{pp\to\tilde{q}\tilde{q}'}$	$K^{DS}_{pp\to\tilde{q}\tilde{q}'}$	$K^{\text{Prospino}}_{pp\to\tilde{q}\tilde{q}'}$
SPS1a	7	1.01 pb	1.37	1.39	1.41
	8	1.48 pb	1.35	1.38	1.40
	14	5.31 pb	1.28	1.34	1.38
10.1.5	7	0.89 fb	1.58	1.58	1.59
	8	2.59 fb	1.53	1.53	1.54
	14	49.87 fb	1.39	1.40	1.41
p19MSSM1A	7	7.65 pb	1.39	1.41	1.37
	8	10.17 pb	1.37	1.41	1.37
	14	28.34 pb	1.31	1.39	1.38

NLO decay

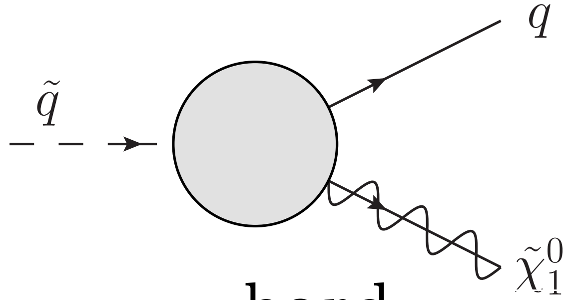

$$d\Gamma^{(1)}_{\tilde{q}\to q\tilde{\chi}^0_j} = d\Gamma^{\text{virtual}}_{\tilde{q}\to q\tilde{\chi}^0_j} + d\Gamma^{\text{soft}}_{\tilde{q}\to q\tilde{\chi}^0_j(g)} + d\Gamma^{\text{coll}}_{\tilde{q}\to q\tilde{\chi}^0_j(g)} + d\Gamma^{\text{hard}}_{\tilde{q}\to q\tilde{\chi}^0_j g}$$

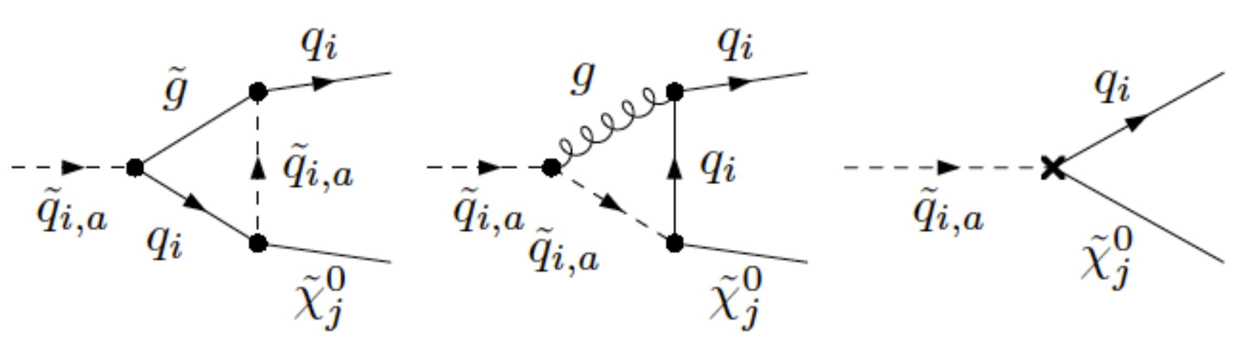

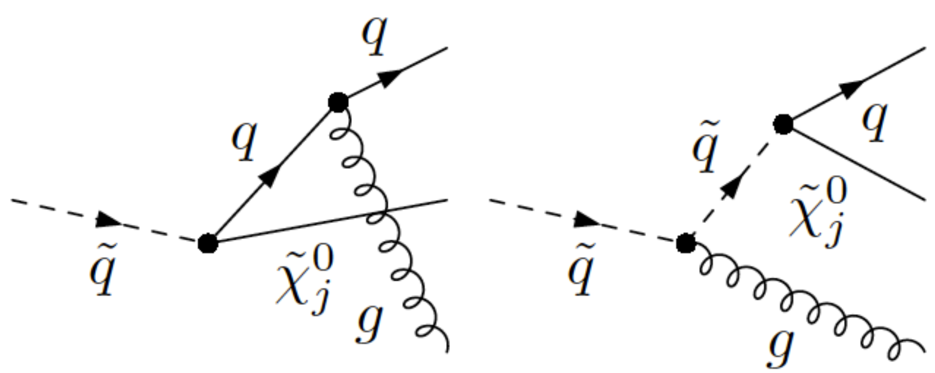

NLO total decay

$$\Gamma^{(0+1)}_{\tilde{q}\to q\tilde{\chi}^0_j} = \Gamma^{(0)}\left[1 + \frac{4}{3}\frac{\alpha_s}{\pi}F^{QCD}\left(\frac{m_{\tilde{\chi}^0_j}}{m_{\tilde{q}}}, \frac{m_{\tilde{q}}}{m_{\tilde{g}}}\right)\right]$$

[Djouadi, Hollik, Jünger; '97]

analytical universal form factor,
recalculated with independent regulators

Benchmark points

benchmarkpoint	m_0	$m_{1/2}$	A_0	$\tan\beta$	sign(μ)
SPS1a	100 GeV	250 GeV	-100 GeV	10	+
10.1.5	175 GeV	700 GeV	0	10	+

benchmarkpoint	M_1	M_2	M_3	A_i	$\tan\beta$	sign(μ)
p19MSSM1A	300 GeV	2500 GeV	360 GeV	0	10	+

benchmarkpoint	$\tilde{u}_L$	$\tilde{u}_R$	$\tilde{d}_L$	$\tilde{d}_R$	$\tilde{g}$	$\tilde{\chi}^0_1$
SPS1a	563.6	546.7	569.0	546.6	608.5	97.0
10.1.5	1437.7	1382.3	1439.7	1376.9	1568.6	291.3
p19MSSM1A	339.6	394.8	348.3	392.7	414.7	299.1

benchmarkpoint		$\tilde{u}_L$	$\tilde{u}_R$	$\tilde{d}_L$	$\tilde{d}_R$	$\tilde{g}$
SPS1a	$\Gamma^{(0)}$	5.361	1.148	5.253	0.287	6.849
	$\Gamma^{(0+1)}$	5.357	1.131	5.255	0.283	
10.1.5	$\Gamma^{(0)}$	12.47	2.854	12.46	0.710	10.04
	$\Gamma^{(0+1)}$	12.31	2.821	12.30	0.702	
p19MSSM1A	$\Gamma^{(0)}$	$2.414 \cdot 10^{-3}$	0.1625	$3.411 \cdot 10^{-3}$	$3.917 \cdot 10^{-2}$	3.441
	$\Gamma^{(0+1)}$	$2.497 \cdot 10^{-3}$	0.1621	$3.503 \cdot 10^{-3}$	$3.912 \cdot 10^{-2}$	

	$\tilde{u}_L$	$\tilde{u}_R$	$\tilde{d}_L$	$\tilde{d}_R$	$\tilde{g}$	$\tilde{l}_L$	$\tilde{l}_R$	$\tilde{\chi}^0_2$	$\tilde{\chi}^0_1$
SPS1a	563.6	546.7	569.0	546.6	608.5	202.4	144.1	180.2	97.0
10.1.6	1531.7	1472.2	1533.6	1466.1	1672.1	536.6	340.6	592.4	313.3

BR (%)	$\tilde{q}_R \to \tilde{\chi}^0_1$	$\tilde{q}_R \to \tilde{\chi}^0_2$	$\tilde{q}_L \to \tilde{\chi}^0_1$	$\tilde{q}_L \to \tilde{\chi}^0_2$	$\tilde{\chi}^0_2 \to \tilde{l}^\pm_L$	$\tilde{\chi}^0_2 \to \tilde{l}^\pm_R$	$\tilde{\chi}^0_2 \to Z$
SPS1a	98.5	1.0	1.5	31.2	–	13.1	-
10.1.6	99.8	0.03	1.5	32.1	28.4	0.2	0.2